

4-11-2019

## Synthesis, Characterization, and Evaluation of Near-IR Boron Dipyrromethene Bioconjugates for Labeling of Adenocarcinomas by Selectively Targeting the Epidermal Growth Factor Receptor

Nichole E.M. Kaufman  
*Louisiana State University*

Qianli Meng  
*Louisiana State University*

Kaitlin E. Griffin  
*Louisiana State University*

Sitanshu S. Singh  
*University of Louisiana at Monroe*

Achyut Dahal  
*University of Louisiana at Monroe*

*See next page for additional authors*

Follow this and additional works at: [https://digitalcommons.lsu.edu/chemistry\\_pubs](https://digitalcommons.lsu.edu/chemistry_pubs)

---

### Recommended Citation

Kaufman, N., Meng, Q., Griffin, K., Singh, S., Dahal, A., Zhou, Z., Fronczek, F., Mathis, J., Jois, S., & Vicente, M. (2019). Synthesis, Characterization, and Evaluation of Near-IR Boron Dipyrromethene Bioconjugates for Labeling of Adenocarcinomas by Selectively Targeting the Epidermal Growth Factor Receptor. *Journal of Medicinal Chemistry*, 62 (7), 3323-3335. <https://doi.org/10.1021/acs.jmedchem.8b01746>

This Article is brought to you for free and open access by the Department of Chemistry at LSU Digital Commons. It has been accepted for inclusion in Faculty Publications by an authorized administrator of LSU Digital Commons. For more information, please contact [ir@lsu.edu](mailto:ir@lsu.edu).

---

## Authors

Nichole E.M. Kaufman, Qianli Meng, Kaitlin E. Griffin, Sitanshu S. Singh, Achyut Dahal, Zehua Zhou, Frank R. Fronczek, J. Michael Mathis, Seetharama D. Jois, and M. Graça H. Vicente



Published in final edited form as:

*J Med Chem.* 2019 April 11; 62(7): 3323–3335. doi:10.1021/acs.jmedchem.8b01746.

## Synthesis, Characterization, and Evaluation of Near-IR Boron Dipyrromethene Bioconjugates for Labeling of Adenocarcinomas by Selectively Targeting the Epidermal Growth Factor Receptor

Nichole E. M. Kaufman<sup>†</sup>, Qianli Meng<sup>†</sup>, Kaitlin E. Griffin<sup>†</sup>, Sitanshu S. Singh<sup>§</sup>, Achyut Dahal<sup>§</sup>, Zehua Zhou<sup>†</sup>, Frank R. Fronczek<sup>†</sup>, J. Michael Mathis<sup>‡</sup>, Seetharama D. Jois<sup>§</sup>, M. Graça H. Vicente<sup>\*,†</sup>

<sup>†</sup>Department of Chemistry, Louisiana State University, Baton Rouge, Louisiana 70803, United States

<sup>‡</sup>Department of Comparative Biomedical Sciences, Louisiana State University School of Veterinary Medicine, Baton Rouge, Louisiana 70803, United States

<sup>§</sup>School of Basic Pharmaceutical and Toxicological Sciences, College of Pharmacy, University of Louisiana at Monroe, Monroe, Louisiana 71201, United States

### Abstract

A series of five boron dipyrromethene (BODIPY) bioconjugates containing an epidermal growth factor receptor (EGFR)-targeted pegylated LARLLT peptide and/or a glucose or biotin ethylene diamine group were synthesized, and the binding capability of the new conjugates to the extracellular domain of EGFR was investigated using molecular modeling, surface plasmon resonance, fluorescence microscopy, competitive binding assays, and animal studies. The BODIPY conjugates with a LARLLT peptide were found to bind specifically to EGFR, whereas those lacking the peptide bound weakly and nonspecifically. All BODIPY conjugates showed low cytotoxicity ( $IC_{50} > 94 \mu M$ ) in HT-29 cells, both in the dark and upon light activation ( $1.5 J/cm^2$ ). Studies of nude mice bearing subcutaneous human HT-29 xenografts revealed that only BODIPY conjugates bearing the LARLLT peptide showed tumor localization 24 h after intravenous administration. The results of our studies demonstrate that BODIPY bioconjugates bearing the EGFR-targeting peptide 3PEG-LARLLT show promise as near-IR fluorescent imaging agents for colon cancers overexpressing EGFR.

\*Corresponding Author: vicente@lsu.edu. Phone: 225-578-7405. Fax: 225-578-3458.

Author Contributions

All authors have given approval to the final version of the manuscript.

Supporting Information

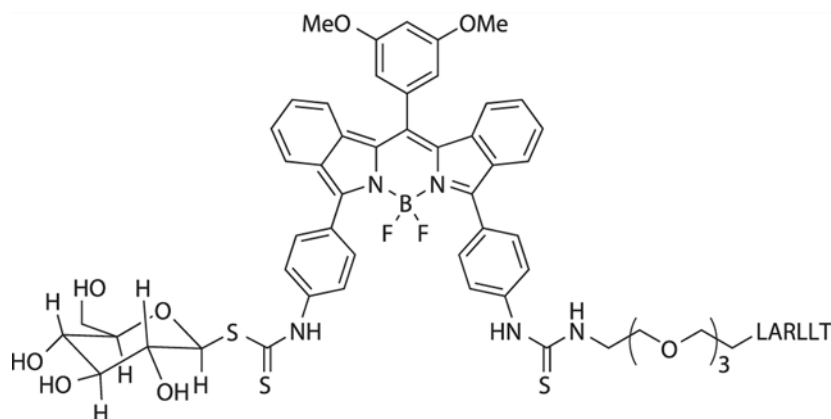
The Supporting Information is available free of charge on the

ACS Publications website at DOI: 10.1021/acs.jmed-chem.8b01746.

Crystallographic data (CIF) for 10 have been deposited at the Cambridge Crystallographic Data Centre, CCD C 1873629 (CSV)

The following files are available free of charge: NMR spectra, MS, HPLC chromatograms, SPR sensorgrams, phototoxicity and dark toxicity plots, and microscopy images (PDF)

The authors declare no competing financial interest.



4,4-Difluoro-4-bora-3a,4a-diaza-*s*-indacene (abbreviated BODIPY or boron dipyrromethene) dyes are versatile small molecules with many desirable characteristics including strong UV-absorption and sharp fluorescence emission peaks, large molar absorption coefficients ( $\epsilon = 50\,000\text{--}100\,000\text{ M}^{-1}\text{ cm}^{-1}$ ), relatively long excited singlet-state

lifetimes ( $> 5$  ns), negligible excited triplet state formation, and high fluorescence quantum yields ( $\Phi > 0.5$ ).<sup>13,17,26</sup> In addition to their excellent photophysical properties, they are relatively stable under physiological conditions and fairly insensitive to changes in polarity and pH of their environment.<sup>13</sup> BODIPY dyes are becoming increasingly useful in the rapidly expanding field of NIR and far-red imaging. Optical and NIR wavelengths typically span from 400 up to 2500 nm, however several tissue components absorb light within this range, making in vivo imaging through tissue difficult. The wavelength range of 650–1450 nm falls in the region of the spectrum with the lowest tissue absorption and with careful design BODIPY can be tuned to both absorb light and emit fluorescence within this long-wavelength “imaging window” of minimal tissue absorbance and minimal autofluorescence.<sup>27</sup>

In 2005 Li et al.<sup>28</sup> reported peptide GE11 (YHWY-GYTPQNVI or EGFR-L2), which was identified through screening of a phage display peptide library. Then, in 2009, Song et al.<sup>31</sup> reported peptide D4 (LARLLT or EGFR-L1) which was discovered using a computer-aided design approach (structure-based peptide design). Both GE11 and D4 peptides show high affinity for the epidermal growth factor receptor (EGFR) both in vitro and in vivo. Our group has previously reported porphyrin,<sup>29</sup> phthalocyanine,<sup>30</sup> and BODIPY<sup>9</sup> fluorophores designed to target EGFR utilizing EGFR-L1, EGFR-L2, and tri-(ethylene)glycol-LARLLT (3PEG-EGFR-L1) with the latter peptide showing the most promise in previous studies because of its improved water solubility and binding resulting in higher intracellular accumulation.<sup>9,29,30</sup> Additionally, enhanced binding was observed in surface plasmon resonance (SPR) studies when two 3PEG-EGFR-L1 peptides were conjugated to a single porphyrin molecule compared with a single 3PEG-EGFR-L1 peptide.<sup>29</sup> This observed binding enhancement may be due to the amphiphilic character of the conjugates with the additional peptide positive charge and/or the potential for binding two, rather than one, EGFR molecules simultaneously.<sup>29</sup> On the basis of this previous work, we envisioned the conjugation of two EGFR targeting 3PEG-EGFR-L1 peptides to a single BODIPY molecule that was tuned to excite and emit in the far-red/near-IR region for the purpose of NIR imaging. On the other hand, the role of saccharides in cell recognition and labeling is well known with several researchers having previously reported the conjugation of multiple carbohydrate units (galactose or lactose) to porphyrin platforms.<sup>16–20</sup> Our group has also reported the conjugation of carbohydrates to BODIPYs, which resulted in increased cellular uptake and permeability.<sup>17</sup> Herein, we report the conjugation of a BODIPY bearing two isocyanato functionalities to the 3PEG-EGFR-L1 peptide, and/or glucose or biotin units. The resulting five conjugates were evaluated in vitro using various cell lines with different EGFR expressions. The most promising BODIPY conjugate bearing one 3PEG-EGFR-L1 and one glucose unit was further evaluated in nude mice bearing subcutaneous human HT-29 xenografts.

## 2. RESULTS AND DISCUSSION

### 2.1. Synthesis and Characterization.

Our group has recently reported the synthesis of a dichlorinated BODIPY bearing a single isothiocyanate functional group, which was used to conjugate EGFR-targeting pegylated

peptides 3PEG-LARLLT and 3PEG-GYHWYGYTPQNVI, in yields of 80 and 50%, respectively.<sup>9</sup> Among these, the BODIPY conjugate bearing the LARLLT peptide was found to have enhanced EGFR-binding ability. On the basis of this work, we decided to synthesize a further red-shifted BODIPY bearing two isothiocyanate functional groups for conjugation to two peptides rather than one or to one peptide and another biomolecule. By inducing a bathochromic shift in both the excitation and emission wavelengths of the BODIPY through functionalization at the 3,5-positions with aryl groups, as well as benzo-fusion to the  $\beta,\beta'$ -pyrrolic positions, we anticipated to lower tissue absorption and increase tissue penetration. The novel incorporation of a second isothiocyanate group to the BODIPY framework affords a second conjugation site for an additional peptide or biomolecule to further enhance tumor selectivity, solubility, and cell permeability.

The precursor BODIPY **10** bearing two *p*-isothiocyanatophenyl groups at the 3- and 5-positions was prepared in nine steps as shown in Scheme 1. The synthetic route to BODIPY **10** began with a Barton–Zard<sup>10</sup> reaction between 1-nitro-cyclohexene and ethyl isocyanoacetate to form the ester functionalized tetrahydro-2*H*-isoindole **2** in 80% yield, using 1,8-diazabicyclo(5.4.0)undec-7-ene (DBU) as a base. This was followed by a Lindsey condensation<sup>11</sup> to form dipyrromethane **3** in 84% yield, using *p*-TsOH as the catalyst.<sup>37,38</sup> Ester cleavage under basic conditions gave dipyrromethane **4**, which underwent decarboxylative iodination under dark conditions to avoid photolytic cleavage of I<sub>2</sub>, in the presence of NaHCO<sub>3</sub> (aq) to yield dipyrromethene **5**. Through a boron complexation reaction, BODIPY **6** was then prepared in 68% yield, by treating dipyrromethene **5** with BF<sub>3</sub>·OEt<sub>2</sub> in the presence of TEA.<sup>13</sup>

With BODIPY **6** in hand, Suzuki–Miyaura coupling was carried out using 5 equiv of 4-nitrophenylboronic acid in the presence of 1 M K<sub>2</sub>CO<sub>3</sub> (aq) using Pd(dppf)Cl<sub>2</sub> as the catalyst,<sup>12</sup> which gave BODIPY **7** in 73–99% isolated yield. Full aromatization of the BODIPY core was achieved with the use of 9 equiv 2,3-dichloro-5,6-dicyano-1,4-benzoquinone (DDQ) in refluxing toluene, monitored by UV/vis, to yield BODIPY **8** in 54–93% yield.<sup>13</sup> Reduction of the aryl nitro groups was carried out with 10 wt % palladium on carbon and hydrazine in a mixture of ethanol and tetrahydrofuran (THF). Finally, conversion of the aryl amines to aryl isothiocyanato groups was accomplished using 1, 1'-thiocarbonyldi-2(1*H*)-pyridone (TDP) in CH<sub>2</sub>Cl<sub>2</sub> to yield BODIPY **10** in 90% yield.<sup>9</sup> The structures of the new BODIPYs were confirmed by <sup>1</sup>H-, <sup>13</sup>C-, and <sup>11</sup>B-NMR and by HRMS [electrospray ionization-time of flight (ESI-TOF)] methodologies (see the Supporting Information).

An adequate single crystal of zaffre blue BODIPY **10** was obtained through slow evaporation of chloroform. X-ray crystallographic analysis unambiguously elucidated a structure in which the BF<sub>2</sub> moiety is disordered into two conformations with approximately 2:1 populations, the F atoms tilted slightly in either direction from symmetric disposition about the central plane. Only one of these is depicted in Figure 1. Interestingly, it was necessary to determine the structure at 180 K because a phase change destroyed the crystal at lower temperatures. The color of the material also changed from blue to emerald green when cooled below the transition temperature. The B–N distances for BODIPY **10** average 1.554(2) Å, which denotes the characteristic delocalization of the positive charge.<sup>32</sup> The

central C<sub>3</sub>N<sub>2</sub>B core of the BODIPY is nearly planar, with mean out-of-plane deviation 0.011 Å. This plane forms dihedral angles of 57.6 and 62.1° with the 3,5-aryl planes and dihedral angle of 78.4° with the meso-aryl plane.

On the basis of our previous studies, peptide 3PEG-LARLLT was selected for conjugation with BODIPY **10**. This peptide was synthesized on Fmoc-Pal-PEG-PS resin using solid-phase peptide synthesis (SPPS), as previously reported.<sup>9,26,29,30,33</sup> In brief, *O*-benzotriazole-*N,N,N',N'*-tetramethyl-uronium-hexafluorophosphate (HBTU), 1-hydroxybenzotriazole (HOBt), and diisopropylethylamine (DIPEA) were utilized as the coupling reagents and a 20% piperidine solution was employed for Fmoc group deprotection. The deprotected peptide was cleaved from the resin using a cocktail solution of trifluoroacetic acid (TFA; 94%), MQ water (2.5%), liquefied phenol (2.5%), and triisopropylsilane (TIPS; 1%), and the cleaved peptide was purified using reversed-phase high-performance liquid chromatography (RP-HPLC). Nucleophilic addition of the purified peptide 3PEG-LARLLT (>95% purity, 2 equiv) was carried out with BODIPY **10** in anhydrous dimethylformamide (DMF) in the presence of TEA, for 30 min at room temperature,<sup>9</sup> affording BODIPY conjugate **11** in 90% yield (Scheme 2). Only one of the isothiocyanato groups of BODIPY **10** reacted with formation of a single thiourea bond. Several attempts were explored to elicit peptide diconjugation, including using a larger excess of peptide and varying the reaction time and concentration of reagents, but no di-peptide substituted BODIPY was observed. Therefore, purified mono-conjugate **11** was treated with 3PEG-LARLLT peptide in anhydrous DMF and TEA, but still no di-peptide BODIPY conjugate was obtained. This result could be due to the initial conjugated peptide adopting a conformation in situ that wraps around the BODIPY, blocking the second isothiocyanate conjugation site.

In an effort to enhance the solubility and receptor binding, the second isothiocyanato functional group was further functionalized with either 1-thio- $\beta$ -D-glucose sodium salt or ethylene diamine-modified biotin (biotin-en), as previously studies reported enhanced cellular permeability and pharmacokinetic properties when these biomolecules were incorporated into the parent molecule.<sup>17,34,35</sup> Therefore, conjugate **11** and 5 equiv of 1-thio- $\beta$ -D-glucose sodium salt or biotin-en were independently solubilized in dimethylsulfoxide (DMSO) and then combined and reacted in the presence of TEA for 30 min at room temperature, yielding conjugates **12** and **13** in 83 and 45% yields, respectively. BODIPY **10** was also reacted with 2.5 equiv of 1-thio- $\beta$ -D-glucose sodium salt or biotin-en, to give the corresponding di-conjugated products, **14** and **15** in 43 and 11% yields, respectively. The bioconjugates **12**, **13**, **14**, and **15** were purified using RP-H PLC, and their structures were characterized using <sup>1</sup>HNMR, heteronuclear single quantum correlation (HSQC), and matrix assisted laser desorption ionization-time of flight mass spectrometry (MALDI-TOF) (see the Supporting Information).

## 2.2. Spectroscopic Investigations.

The spectroscopic properties of BODIPY bioconjugates **11–15** in DMSO, including their maximum absorption and emission wavelengths, Stokes' shifts, fluorescence quantum yields, and molar extinction coefficients, were investigated, and the results are summarized in Table 1. Figures S22 and S23 of the Supporting Information show the normalized



absorption and emission spectra for the bioconjugates. All compounds showed  $\pi \rightarrow \pi^*$  absorption bands between 650 and 657 nm and emission wavelengths in the NIR range between 689 and 696 nm in DMSO. The Stokes' shifts for all compounds were between 38 and 40 nm, and the molar extinction coefficients ( $\epsilon$ ) ranged from 13 700 to 72 600 M<sup>-1</sup> cm<sup>-1</sup>, as is characteristic for BODIPY-peptide conjugates. All compounds showed fluorescence quantum yields ( $\Phi_F$ ) in the range of 0.37–0.47 in DMSO.

All BODIPY bioconjugates were soluble in polar organic solvents, such as DMSO. Their polar surface area (PSA) values, which measure their solvent-accessible surface area, were calculated and the results are also shown in Table 1. The peptide-containing conjugates showed similar PSA values, indicating that they have similar cellular permeability.

### 2.3. SPR Studies.

SPR was used to determine the binding affinities of compounds **10** and **11–14** with EGFR protein ECD because it allows real-time, label-free detection of biomolecular interactions.<sup>14,15</sup> Sensorgrams of binding of BODIPYs **12** and **13** are shown in Figure 2 (the sensorgrams for BODIPYs **10,11**, and **14** are shown in Figure S25B,C,A of the Supporting Information). BODIPYs **12** and **13** both exhibited a stepwise binding to EGFR ECD with kinetics of association of 200 s and dissociation for the next 300 s. The sensorgrams indicated a slow increase in response with saturation behavior suggesting that binding of these BODIPYs is specific to EGFR ECD. Similar results were observed for BODIPY **11** (Figure S25C of the Supporting Information). In the case of BODIPY **14** (Figure S25A, Supporting Information), binding or association was rapid, as there was a very steep increase in the association phase and slow dissociation phase. Furthermore, at high concentration (250  $\mu$ M), there was a decrease in response compared with that at 100  $\mu$ M. For the bis-NCS BODIPY **10** (Figure S25B, Supporting Information), the sensorgrams were not stepwise upon addition of different concentrations of compound, suggesting nonspecific binding or weak binding of this BODIPY. The dissociation constants ( $K_D$ ) were also calculated using a 1:1 binding fit with  $K_D$  values of  $2.635 \times 10^{-3}$  and  $3.083 \times 10^{-6}$  M for **12** and **13**, respectively (Table S1 in Supporting Information). Overall, the SPR studies clearly indicated that the BODIPYs conjugated with peptide 3PEG-LARLLT exhibited specific binding to EGFR ECD while the BODIPYs lacking peptide, **10** and **14**, bound to EGFR nonspecifically.

### 2.4. Modeling and Docking.

To model the interaction of BODIPYs **11–15** with EGFR, three-dimensional structures of these conjugates, as well as of BODIPY **10**, were generated, and the 3D structures of the conjugates were docked to the EGFR closed conformation using AutoDock.<sup>39</sup> The results of these studies are shown in Figure 3 for BODIPYs **12** and **14** (and Figure S26C, D, A, B of the Supporting Information for BODIPYs **10, 11, 13**, and **15**). Peptide LARLLT is known to bind to domain I of EGFR, away from the EGF binding pocket,<sup>31</sup> and thus, BODIPYs **10–15** were docked on domain I of EGFR. Conjugate **13** was found to bind near the LARLLT peptide binding pocket, with three possible hydrogen bonds and hydrophobic interactions. Residue T6 of the peptide formed hydrogen bonds with Glu78 and Asn79. The aromatic groups of BODIPY were involved in hydrophobic interactions with Leu225, Lys185,



Pro171, Ile189 and 190, and Lys202 side chains. The biotin-en groups formed a hydrogen bond interaction with Arg200. Furthermore, the PEG linker of the peptide, R3 side chain, and backbone amides of L6 formed polar interactions with Gln78, Asn79, Glu35, Gln59, and Gln81 of EGFR. Overall, the peptide structure was stabilized on domain I of EGFR binding pocket with a docking energy of  $-4.21$  kcal/mol. BODIPY conjugates **11** (Figure S26D) and **12** (Figure 3), also containing one LARLLT peptide, formed similar interactions with domain I of EGFR as described above for **13**. In the case of BODIPY **12** (Figure 3), the glucose moiety formed additional hydrogen bond interactions with Arg200 of EGFR. Docking energies for BODIPYs **11** and **12** were  $-4.73$  and  $-4.00$  kcal/mol, respectively, which are within the calculation error of up to 2 kcal/mol. On the other hand, BODIPYs **14** (Figure 3), **15** (Figure S26B), and **10** (Figure S26C), bearing no peptide, appear to bind nonspecifically to EGFR. Docking studies indicated that there are two possible binding sites for these BODIPYs, with the lowest energy docked structures located in a buried hydrophobic pocket away from the binding site defined for the LARLLT peptide. The second possible binding site was near Pro171, Ile189, 190, and Lys202. For BODIPY **10**, all of the possible binding sites were away from the LARLLT binding pocket on EGFR. The lowest docking energies for BODIPYs **14**, **15**, and **10** were found to be  $-8.4$ ,  $-8.9$ , and  $-11.1$  kcal/mol, respectively. The docking energy depends on how deeply buried a molecule is, as well as the number of rotatable bonds in the molecule. Because the BODIPYs without peptide were mostly hydrophobic with rigid aromatic structures, the docking energy was lower than that for the BODIPYs containing the LARLLT peptide. These results are consistent with the SPR data which suggest that the peptide-containing BODIPYs **11**, **12**, and **13** bind to domain I of EGFR, while BODIPYs **10**, **14**, and **15** containing no peptide bind nonspecifically in deep hydrophobic binding pockets on EGFR.

## 2.5. In Vitro Studies.

Several cell lines with different expressions of EGFR were used to investigate the cell membrane localization, uptake, and cytotoxicity of BODIPY conjugates **12**, **13**, **14**, and **15**. The human colorectal adenocarcinoma cell line HT-29 is considered a pluripotent intestinal cell line and is widely used to study the biology of human cancers.<sup>5</sup> Human colon cancer cell lines SW480 (129% EGFR expression), HT-29 (78% EGFR expression), DLD-1 (37% EGFR expression), and LOVO (6% EGFR expression) were purchased from the American Type Culture Collection (ATCC) (Manassas, Virginia, USA) and chosen to ensure that a full spectrum of cell surface EGFR expression was examined.<sup>8</sup>

**2.5.1. Competitive Binding Studies.**—The specificity of BODIPY binding to EGFR on colon cancer cells was investigated by competitive binding of conjugates **12** and **14** with unlabeled cyclo(K(N<sub>3</sub>)larllt) peptide,<sup>21</sup> which has been shown to bind to EGFR with high affinity. The results obtained are shown in Figures 4 and S27 (the Supporting Information). The colon cancer cell lines SW480 (high EGFR expression), HT-29 and DLD-1 (moderate EGFR expression), and LOVO (low EGFR expression) were used in these studies.<sup>8</sup> When BODIPY **12** ( $50\ \mu\text{M}$ ) was incubated with unlabeled cyclic peptide at concentrations up to  $100\ \mu\text{M}$ , a dose-dependent decrease in fluorescence was observed in the cell lines with high and moderate EGFR expression but not in LOVO cells (Figure 4). The highest inhibition of fluorescence intensity was observed in the SW480 cell line with the highest expression of

EGFR, followed by HT-29 and DLD-1 cells, indicating the replacement of unlabeled peptide specifically in the high EGFR expressing cells. On the other hand, the incubation of unlabeled peptide with BODIPY **12** in LOVO cells, with low EGFR expression, did not result in a concentration-dependent response of the fluorescence intensity. A decrease in fluorescence was nevertheless observed upon addition of unlabeled cyclic peptide, suggesting some nonspecific binding of the conjugate to the LOVO cells. Similar studies were carried out with BODIPY **14**, which contains two glucose units and bears no EGFR-targeting LARLLT peptide. In this case, competitive binding of **14** in the presence of unlabeled cyclic peptide, led to no concentration-dependent response of the fluorescence intensity in all four cell lines, although a decrease in fluorescence was observed upon addition of unlabeled cyclic peptide. This result suggests some nonspecific binding of conjugate **14** (Figure S27, the Supporting Information). These results are in agreement with the SPR studies and indicate that BODIPYs bearing the LARLLT peptide bind to EGFR specifically, whereas BODIPYs without peptide bind to EGFR nonspecifically.

**2.5.2. Time-Dependent Cellular Uptake.**—The uptake BODIPYs **12**, **13**, **14**, and **15** by human colorectal adenocarcinoma HT-29 cells was investigated at a concentration of 10  $\mu\text{M}$  over a 24 h period. Figure 5 shows the results obtained in these studies. BODIPYs **12** and **13** bearing the LARLLT peptide showed similar uptake kinetics with rapid accumulation in the first 8 h, after which a plateau was reached. BODIPY **12** accumulated the most within cells of all BODIPYs up to 12 h, but at 24 h, the bis-biotin conjugate **15** showed the highest uptake of all. This is due to the continuous increasing in the uptake of **15** over the 24 h period investigated. At all time points investigated, BODIPY **12** showed higher uptake than **13** because of the presence of glucose in **12** in place of the biotin group in **13**, suggesting that glucose enhances the cellular uptake. However, BODIPY **14** bearing two glucose units accumulated the least within cells of all BODIPYs. These results indicate that because the glucose groups modulate the hydrophobic character of the conjugates, one glucose leads to an amphiphilic molecule with enhanced cellular uptake, whereas two glucoses lead to a more hydrophilic conjugate with decreased uptake. On the other hand conjugate **15** containing two biotin groups showed continued uptake over the 24 h period, suggesting a different cellular uptake mechanism from BODIPYs **12** and **13** bearing the EGFR-targeting peptide.

**2.5.3. Cytotoxicity.**—The cytotoxicity of BODIPYs **12**, **13**, **14**, and **15** was evaluated in human colorectal adenocarcinoma HT-29 cells using a CellTiter Blue (CTB) assay. The results of these studies are shown in Table 2 (and Figures S28 and S29 of the Supporting Information). The BODIPY conjugates were analyzed at up to 200  $\mu\text{M}$  concentrations for dark toxicity and at up to 100  $\mu\text{M}$  concentrations for phototoxicity using a low light dose of approximately 1.5 J/cm<sup>2</sup>. In the dark toxicity studies, all four BODIPY conjugates showed a moderate decrease in cell toxicity with increasing concentration, as shown in Figure S28. BODIPY **14** showed the lowest cytotoxicity of all conjugates, with approximately 80% cell survival at 200  $\mu\text{M}$ , whereas BODIPY **13** displayed the highest cytotoxicity with approximately 40% cell survival at 200  $\mu\text{M}$ . The IC<sub>50</sub> values, calculated from the dose response curves, were 159  $\mu\text{M}$  for **13** and above 200  $\mu\text{M}$  for all other BODIPYs. Bioconjugates **12** and **13** showed lower cell survival rates across the concentration range

compared with **14** and **15**, which may be a result of the greater accumulation of **12** and **13** in cells because of the presence of the cationic EGFR-targeting peptide LARLLT. For phototoxicity studies, a low light dose ( $1.5 \text{ J/cm}^2$ ) was used and the results are shown in Figure S29 and summarized in Table 2. The BODIPYs were found to have low phototoxicities, with  $\text{IC}_{50}$  values above  $100 \mu\text{M}$ , except for **12** that was found to have an  $\text{IC}_{50}$  value of  $94 \mu\text{M}$ . The higher observed cytotoxicity of BODIPY **12** might be a result of its higher uptake into the HT-29 cells (Figure 5). Among all BODIPYs, conjugate **14** appears to be the least phototoxic, which may be attributed to the observed reduced cellular uptake for this compound. Overall, all BODIPY bioconjugates showed low cytotoxicities, making them promising candidates as fluorescent bioimaging agents.

**2.5.4. Extracellular Localization.**—The extent of extracellular localization of the BODIPY conjugates was evaluated by fluorescence microscopy, and the results are shown in Figures 6 and S30 of the Supporting Information. The SW 480 cells (highest EGFR expression) and LOVO cells (lowest EGFR expression) were used in these studies. Both cell lines were independently exposed to BODIPY conjugates **12**, **13**, **14**, and **15** at a concentration of  $10 \mu\text{M}$  for 15 min, immediately followed by imaging. With BODIPYs **12** and **13**, a significantly higher fluorescence signal was observed in the SW480 cells compared with the LOVO cells, indicating that these compounds are actively binding to the ECD of EGFR overexpressed in the SW480 cells. A weaker fluorescence signal was also observed in the case of BODIPYs **14** and **15**, suggesting nonspecific binding of these compounds to the EGFR overexpressing cells. These findings are in agreement with the results obtained in the SPR and AutoDock model studies.

## 2.6. In Vivo Studies.

BODIPYs **12** and **14** were selected for evaluation in nude mice bearing HT-29 subcutaneous tumors on the lower right flank, and the results are shown in Figure 7. BODIPY **12** containing the EGFR-targeting peptide LARLLT was selected because of its rapid cellular uptake, low cytotoxicity, EGFR-targeting ability, and good solubility, whereas BODIPY **14** was selected as a negative control. Nude mice were administered  $100 \mu\text{L}$  of 2 mM BODIPY **12** or **14** via lateral tail vein injection, followed by fluorescence imaging at 0, 24, 48, 72, and 96 h post-injection. At time 0, the fluorescence of both compounds can clearly be seen localized in the tail, and in the case of **12**, immediate plasma circulation was observed. At 24 h, the mouse administered BODIPY **12** clearly showed tumor-selective fluorescence indicating that this conjugate targeted the subcutaneous tumor tissue, while the signal from **14** was significantly weaker. The fluorescence signal progressively decreased with time, indicating slow clearance of the BODIPY at 48, 72 and 96 h, with the highest signal at these time points still within the tumor tissue. For BODIPY **14**, minimal fluorescence was observed suggesting no EGFR-targeting ability for this conjugate.

## 3. CONCLUSIONS

A near-IR BODIPY bearing two isothiocyanato functional groups available for conjugation to an EGFR-targeting peptide and/or water-solubilizing moiety was synthesized. On the basis of previous studies, the peptide 3PEG-LARLLT was selected for EGFR-targeting, and

glucose or biotin-en were selected for enhanced solubility of the conjugates. Five BODIPY conjugates were prepared and characterized, three of them bearing one 3PEG-LARLLT peptide and one or no water-solubilizing glucose or biotin group. Using AutoDock, all conjugates were found to bind to EGFR with negative docking energies but only the peptide-containing conjugates were able to bind to the known binding site of the LARLLT peptide, on the ECD I of EGFR.

SPR studies indicated that BODIPY conjugates **12** and **13** bearing the EGFR-targeting peptide exhibited specific binding to the ECD of EGFR compared with conjugates **14** and **15**, both devoid of peptide, which showed only nonspecific binding to EGFR. This was confirmed by fluorescence microscopy studies, which revealed higher extracellular fluorescence in the high EGFR expressing cell line SW480 compared with the low EGFR expression cell line LOVO, using conjugates **12** and **13**. Competitive binding studies revealed a dose-dependent decrease in fluorescence in cells with high and moderate EGFR expression for conjugate **12**, whereas **14** was found to have no dose-dependent response, indicating nonspecific binding to EGFR. In vitro cytotoxicity studies showed no significant dark nor phototoxicity in human colorectal adenocarcinoma HT-29 cells for any of the BODIPY conjugates. BODIPYs **12** and **13** containing the EGFR-targeting peptide, displayed similar uptake kinetics in HT-29 cells, distinct from those of conjugates **14** and **15**, with **12** accumulating the most within cells in the first 12 h.

BODIPYs **12** and **14**, bearing one or no EGFR-targeting peptide, respectively, were investigated in nude mice bearing HT-29 human tumor xenografts. Conjugate **12** showed the highest fluorescence signal at the site of the subcutaneous tumor at 24 h after iv administration, and the signal was still visible at 48, 72, and 96 h post-injection, indicating slow clearance from the body. On the other hand, BODIPY **14** bearing two glucose units exhibited a much reduced fluorescence signal at the tumor site. Our results show that BODIPY **12** exhibits high selectivity for the ECD of EGFR, low cytotoxicity, and good aqueous solubility and is therefore a promising candidate for imaging of EGFR-overexpressing tumors.

## 4. EXPERIMENTAL SECTION

### 4.1. General Information.

All reagents and solvents were purchased from Sigma-Aldrich (St Louis, MO) or VWR (Radnor, PA) and used without further purification unless otherwise stated. Dry solvents were obtained from a Solvent Purification System Pure Solv PS-400 (Innovative Technology, Carouge Switzerland). Melting points were determined in open capillary tubes and are reported as is. Reactions were monitored using polyester backed 0.2 mm silica G thin-layer chromatography (TLC) plates (Sorbent Technologies, Norcross GA), and column chromatography was performed using 60 Å, 40–63  $\mu$ M silica gel (Sorbent Technologies, Norcross GA). All  $^1\text{H}$  NMR,  $^{11}\text{B}$  NMR, and  $^{13}\text{C}$  NMR spectra were collected using a Bruker AVANCE III 400 MHz spectrometer or AVANCE III 500 MHz spectrometer equipped with Prodigy TCI probe. Samples were dissolved in either deuterated chloroform ( $\text{CDCl}_3$ ) or DMSO( $\text{DMSO}-d_6$ ) using tetramethylsilane as an internal standard. Chemical

shifts ( $\delta$ ) are reported in ppm where  $\text{CDCl}_3$  ( $^1\text{H}$ : 7.27 ppm,  $^{13}\text{C}$ : 77.0 ppm) and  $\text{DMSO}-d_6$  ( $^1\text{H}$ : 2.50 ppm) are used as references. Coupling constants ( $J$ ) are reported in Hertz (Hz). BODIPY conjugates were purified using RP-HPLC composed of a 2489 UV/vis detector, a 2545 quaternary gradient module pump and a FlexInject sample injector (Waters, Milford MA) to a purity of 95% (unless otherwise noted). Separations were achieved on an X-Bridge BEH300 Prep C18 column (5  $\mu\text{m}$ , 10  $\times$  250 mm) equipped with an X-Bridge BEH300 Prep guard column (300  $\text{\AA}$ , 5  $\mu\text{m}$ , 10  $\times$  10 mm) using a gradient of 50% A for 5 min, 30% A to 10% A over 13 min, 10% A to 50% A over 2 min at a flow rate of 4 mL/min (unless otherwise noted) and analyzed with Empower 2 software. HRMS were obtained using an Agilent 6210 ESI-TOF mass spectrometer (Agilent Technologies, Santa Clara CA) or MALDI-TOF ultrafleXtreme mass spectrometer (Bruker, Billerica, MA).

#### 4.2. Synthesis of 2-Ethoxycarbonyl-4,5,6,7-tetrahydro-2H-isoindole 2.

1-nitro-1-cyclohexene **1** (1.13 g, 8.89 mmol) and ethyl isocyanoacetate (1.04 g, 9.15 mmol) were dissolved in THF (10–15 mL), and then, DBU (1.73 g, 11.38 mmol) was added and the solution was allowed to stir overnight at room temperature under an inert atmosphere. Next, the reaction mixture was washed with brine and extracted with DCM. The combined organic layers were dried over  $\text{Na}_2\text{SO}_4$ , and all solvents were removed under reduced pressure. The resultant residue was purified by means of column chromatography using ethyl acetate/hexanes 1:9 as the eluent to afford compound **2** as a pale yellow solid (1.37 g, 80%). The spectroscopic data of this compound agree with that previously reported.<sup>36</sup>

#### 4.3. Synthesis of 8-(3,5-Dimethoxyphenyl)-bis(3-ethoxycarbonyl-4,5,6,7-tetrahydro-2H-isoindolyl)methane 3.

2-Ethoxycarbonyl-4,5,6,7-tetrahydro-2H-isoindole **2** (0.77 g, 3.98 mmol), 3,5-dimethoxybenzaldehyde (0.331 g, 1.99 mmol), *p*-TsOH (0.017 g, 0.996 mmol), and *tert*-butylammonium iodide (40 mg) were dissolved in DCM (100 mL) and allowed to stir overnight at room temperature. The reaction mixture was then washed with saturated  $\text{NaHCO}_3$  and extracted with DCM. The combined organic layers were dried over  $\text{Na}_2\text{SO}_4$ , and the solvent was removed under reduced pressure. The resultant residue was purified by column chromatography using ethyl acetate/hexanes 1:5 as the eluent to afford bright orange crystals of compound **3** (0.899 g, 84%). mp 89–90 °C;  $^1\text{H}$  NMR (400 MHz,  $\text{CDCl}_3$ ):  $\delta$  9.39 (s, 2H), 6.33 (t,  $J$  = 2.3 Hz, 1H), 6.24 (d,  $J$  = 2.3 Hz, 4H), 5.40 (s, 1H), 4.19–4.09 (m, 4H), 3.67 (s, 6H), 2.76 (t,  $J$  = 6.3 Hz, 4H), 2.27 (t,  $J$  = 6.3 Hz, 1H), 1.73–1.64 (m, 8H), 1.24 (t,  $J$  = 7.1 Hz, 6H); HRMS (ESI-TOF)  $m/z$ : calcd for  $\text{C}_{31}\text{H}_{39}\text{N}_2\text{O}_6$ , 535.2803; found  $[\text{M} + \text{H}]^+$ , 535.2811.

#### 4.4. Synthesis of 8-(3,5-Dimethoxyphenyl)-bis(3-carboxyl-4,5,6,7-tetrahydro-2H-isoindolyl)methane 4.

Compound **3** (0.800 g, 1.50 mmol) was dissolved in THF (6 mL) and methanol (6 mL), followed by addition of KOH solution (0.840 g, 14.9 mmol) in water (10 mL). The solution was refluxed at 90–100 °C for 24 h and then allowed to cool to room temperature. A 1 M solution of HCl was added to the mixture until pH of 5 was reached. The reaction mixture was filtered and the light pink-purple precipitate was collected. For compound **4**,  $^1\text{H}$  NMR

(400 MHz, CDCl<sub>3</sub>):  $\delta$  8.75 (m, 2H), 6.37 (t,  $J$  = Hz, 1H), 6.26 (d,  $J$  = Hz, 2H), 5.34 (s, 1H), 4.21 (m, 4H), 3.72 (s, 6H), 2.79 (t,  $J$  = Hz, 4H), 2.22 (t,  $J$  = Hz, 4H), 1.69 (m, 8H), 1.30 (t,  $J$  = Hz, 6H).

#### 4.5. Synthesis of 8-(3,5-Dimethoxyphenyl)-bis(3-iodo-4,5,6,7-tetrahydro-2H-isoindolyl)methene 5.

Compound 4 (0.900 g, 1.88 mmol) was dissolved in methanol (40 mL) in a round-bottom flask (RBF) followed by addition of sodium bicarbonate (1.58 g, 18.8 mmol) and distilled water (15 mL). The RBF was then wrapped in aluminum foil to prevent light penetration followed by addition of iodine (1.43 g, 5.64 mmol). The reaction mixture was allowed to stir at room temperature for 72 h. The solution was then cooled in an ice bath, and stirring was ceased. The solid was filtered, washed with cold distilled water, then dissolved in DCM, and washed with saturated Na<sub>2</sub>S<sub>2</sub>O<sub>3</sub>. The combined organic layers were dried over Na<sub>2</sub>SO<sub>4</sub>, and the solvent was removed under reduced pressure. The residue was purified using column chromatography to afford a maroon solid. For compound 5, <sup>1</sup>H NMR (400 MHz, CDCl<sub>3</sub>):  $\delta$  9.08 (s, 1H), 6.65 (d,  $J$  = 2.76, 2H), 4.31 (dd,  $J$  = 7.12 Hz, 4H), 2.83 (t,  $J$  = Hz, 4H), 2.56 (t,  $J$  = Hz, 4H), 1.75 (m, 8H), 1.35 (t,  $J$  = Hz, 6H).

#### 4.6. Synthesis of 3,5-Diiodo-8-(3,5-dimethoxyphenyl)-BODIPY 6.

Compound 5 (1.20 g, 1.87 mmol) was dissolved in DCM (100 mL) and allowed to stir under nitrogen. Triethylamine (TEA; 1.90 g, 28.1 mmol) was added followed by BF<sub>3</sub>·OEt<sub>2</sub> (3.99 g, 28.11 mmol), and the reaction was allowed to stir at room temperature for 2 h. Subsequently, the solvent was removed under reduced pressure and the resultant residue was solubilized in ethyl acetate and washed with 1 M HCl followed by saturated NaHCO<sub>3</sub>. The combined organic layers were dried over Na<sub>2</sub>SO<sub>4</sub>, and the solvent was removed under reduced pressure. The residue was then purified by column chromatography using DCM/hexanes 2:1 as the eluent to afford compound 6 as a bright pink crystalline solid (0.877 g, 68%), mp 226–227 °C; <sup>1</sup>H NMR (400 MHz, CDCl<sub>3</sub>):  $\delta$  6.55 (t,  $J$  = 2.3 Hz, 1H), 6.39 (d,  $J$  = 2.3 Hz, 2H), 3.80 (s, 6H), 2.31 (t,  $J$  = 6.2 Hz, 4H), 1.74 (t,  $J$  = 6.2 Hz, 4H), 1.65–1.59 (m, 4 h); HRMS (ESI-TOF)  $m/z$ : calcd for C<sub>25</sub>H<sub>24</sub>BF<sub>2</sub>N<sub>2</sub>O<sub>2</sub>, 668.0113; found [M–F]<sup>+</sup>, 668.0098.

#### 4.7. General procedure for Synthesis of 8-(3,5-Dimethoxyphenyl)-bis(3-*p*-nitrophenyl)-BODIPY 7.

BODIPY 6 (0.150 g, 218.0 mmol), 4-nitrophenylboronic acid (0.182 g, 1.09 mmol), and a catalytic amount of [1,1'-bis(diphenylphosphino)ferrocene]-palladium(II) dichloride (Pd(dppf)Cl<sub>2</sub>) were added to an RBF under nitrogen atmosphere. THF (2–33 mL) and toluene (2–3 mL) were added, and the solution was heated to 70–80 °C followed by addition of 1 M K<sub>2</sub>CO<sub>3</sub> (2.18 mL). The reaction was allowed to stir for 3 h. Subsequently, all solvents were removed under reduced pressure, and the resultant residue was purified by column chromatography using DCM/hexanes 3:1 as the eluent to afford compound 7 as a deep purple crystalline solid (134.6 mg, 91%), <sup>1</sup>H NMR (400 MHz, CDCl<sub>3</sub>):  $\delta$  8.27–8.20 (m, 4H), 7.76–7.69 (m, 4H), 6.62 (t,  $J$  = 2.3 Hz, 1H), 6.53 (d,  $J$  = 2.2 Hz, 2H), 3.87 (s, 6H), 2.29 (t,  $J$  = 6.0 Hz, 4H), 1.93 (t,  $J$  = 6.1 Hz, 4H), 1.55 (d,  $J$  = 7.5 Hz, 8H), HRMS (ESI-TOF)  $m/z$ : calcd for C<sub>37</sub>H<sub>33</sub>BF<sub>2</sub>N<sub>4</sub>O<sub>6</sub>, 677.2492; found [M]<sup>+</sup>, 677.2440.



**4.8. Synthesis of 8-(3,5-dimethoxyphenyl)-bis(3-*p*-nitrophenyl)-BODIPY 8.**

BODIPY 7 (0.135 g, 199.0 mmol) was solubilized in toluene (20 mL) followed by addition of DDQ (0.407 g, 1.79 mmol). The reaction mixture was refluxed for 1.5 h, and the reaction was followed by UV/vis. The solvent was removed under reduced pressure and washed with saturated NaHCO<sub>3</sub>. The combined organic layers were dried over Na<sub>2</sub>SO<sub>4</sub> and solvent was removed under reduced pressure. The resultant residue was purified by column chromatography using DCM/hexanes 3:1 as the eluent to afford compound 8 as a purple crystalline solid (124.1 mg, 93%), <sup>1</sup>H NMR (400 MHz, CDCl<sub>3</sub>): δ 8.40–8.33 (m, 4H), 8.00–7.92 (m, 4H), 7.55–7.46 (m, 2H), 7.26–7.18 (m, 4H), 6.85 (t, *J* = 2.3 Hz, 2H), 6.60–6.52 (m, 2H), 3.89 (s, 6H); HRMS (ESI-TOF) *m/z*: calcd for C<sub>37</sub>H<sub>26</sub>BF<sub>2</sub>N<sub>4</sub>O<sub>6</sub>, 670.194; found [M + H]<sup>+</sup>, 670.1954.

**4.9. Synthesis of 8-(3,5-dimethoxyphenyl)-bis(3-*p*-amino-phenyl)-BODIPY 9.**

BODIPY 8 (0.0661 g, 0.0986 mmol) and palladium on carbon (0.262 g) were added to an RBF followed by addition of ethanol (5–7 mL), THF (4–5 mL), and hydrazine (0.494 g, 9.86 mmol). The reaction mixture was refluxed for 2–3 h and followed by TLC. Next, all solvents were removed under reduced pressure, and the residue was solubilized in DCM and passed through a celite cake. The filtrate was collected and solvent was removed under reduced pressure. The resultant residue was purified by column chromatography using ethyl acetate/DCM 1:1 as the eluent to afford a dark blue solid. <sup>1</sup>H NMR (400 MHz, CDCl<sub>3</sub>): δ 7.62–7.60 (d, *J* = 7.3 Hz, 6H), 7.12 (m, 4H), 6.81–6.79 (d, *J* = 7.9 Hz, 7H), 6.52–6.50 (d, *J* = 7.28 Hz, 2H), 4.11–4.05 (dd, *J* = 14.4, 7.1 Hz, 4H), 3.85 (s, 6H); HRMS (ESI-TOF) *m/z*: calcd for C<sub>37</sub>H<sub>29</sub>BF<sub>2</sub>N<sub>4</sub>O<sub>2</sub>, 590.2398; found [M – F]<sup>+</sup>, 590.2399.

**4.10. Synthesis of 8-(3,5-Dimethoxyphenyl)-bis(3-*p*-isothio-cyanato phenyl)-BODIPY 10.**

BODIPY 9 (0.0602 g, 0.0986 mmol) was dissolved in DCM (10 mL) followed by addition of TDP (0.0916 g, 0.349 mmol), and the reaction mixture was allowed to stir overnight at room temperature under an inert atmosphere. The solvent was then removed under reduced pressure, and the resultant residue was purified by column chromatography using DCM/hexane 2:1 as the eluent to afford compound 10 as a dark blue crystalline solid (54.2 mg, 90%), mp 222–223 °C; <sup>1</sup>H NMR (400 MHz, CDCl<sub>3</sub>): δ 7.79 (d, *J* = 8.5 Hz, 4H), 7.51 (m, 2H), 7.36 (d, *J* = 8.5 Hz, 4H), 7.16 (td, *J* = 6.8, 6.1, 3.4 Hz, 4H), 6.80 (dd, *J* = 13.6, 2.3 Hz, 3H), 6.51 (m, 2H), 3.86 (s, 6H); <sup>13</sup>C NMR (125 MHz, CDCl<sub>3</sub>): δ 162.10, 150.27, 136.95, 136.70, 136.67, 134.37, 132.53, 1313.82, 131.79, 131.76, 131.07, 131.05, 131.03, 130.10, 129.54, 126.78, 125.83, 125.47, 123.20, 122.12, 106.76, 102.22, 77.42, 55.91, 29.90; <sup>11</sup>B-NMR (128 MHz, CDCl<sub>3</sub>): δ 1.68 (t, *J*<sub>BF</sub> = 30.7 Hz). HRMS (ESI-TOF) *m/z*: calcd for C<sub>39</sub>H<sub>25</sub>BF<sub>2</sub>N<sub>4</sub>O<sub>2</sub>S<sub>2</sub>, 694.1589; found [M + H]<sup>+</sup>, 694.1542.

**4.11. Synthesis of Biotin-en.**

Commercially obtained biotin (0.0500 g, 0.205 mmol), N-(3-dimethylaminopropyl)-N'-ethylcarbo-diimide hydrochloride (0.0953 g, 0.614 mmol), and HOBt (0.830 g, 0.614 mmol) were solubilized in DMSO (2 mL) followed by addition of TEA (0.0621 g, 0.614 mmol), and the reaction mixture was allowed to stir at room temperature for 1–2 h. Then, *N*-Boc-ethylenediamine (0.492 g, 0.307 mmol) was added, and the reaction mixture was allowed to



stir at room temperature for 12 h. The reaction mixture was extracted in DCM and washed in series with saturated  $\text{NH}_4\text{Cl}$ , followed by saturated  $\text{NaHCO}_3$  and finally with brine. The combined organic layers were dried over  $\text{Na}_2\text{SO}_4$ , and all solvents were removed under reduced pressure. The resultant residue was then purified by column chromatography using DCM/methanol 9:1 as the eluent to afford the corresponding *N*-Boc-protected biotin as a pearl white solid (38.0 mg, 48%), HRMS (ESI-TOF)  $m/z$ : calcd for  $\text{C}_{17}\text{H}_{31}\text{N}_4\text{O}_4\text{S}$ , 387.2061; found  $[\text{M} + \text{H}]^+$ , 387.2056. This compound (0.0322 g, 0.0833 mmol) was solubilized in 20% TFA in DCM (2 mL) and allowed to stir at room temperature for 2 h. The reaction mixture was washed with diethyl ether to remove residual TFA, and all solvents were removed under reduced pressure to afford compound **12** as an off-white solid.  $^1\text{H}$  NMR (400 MHz,  $\text{CDCl}_3$ ):  $\delta$  7.77 (t,  $J$  = 5.6 Hz, 1H), 6.77 (t,  $J$  = 5.8 Hz, 1H), 6.41 (s, 2H), 4.30 (dd,  $J$  = 7.7, 5.1 Hz, 1H), 4.12 (ddd,  $J$  = 7.5, 4.5, 1.7, Hz, 1H), 3.07 (m, 3H), 2.95 (q,  $J$  = 6.4 Hz, 2H), 2.82 (dd,  $J$  = 12.4, 5.1 Hz, 1H), 2.57 (d,  $J$  = 12.4 Hz, 3H), 2.04 (t,  $J$  = 7.4 Hz, 2H), 1.68–1.40 (m, 5H), 1.37 (s, 10H), 1.33–1.13 (m, 5H); HRMS (ESI-TOF)  $m/z$ : calcd for  $\text{C}_{12}\text{H}_{23}\text{N}_4\text{O}_2\text{S}$ , 287.1536; found  $[\text{M} + \text{H}]^+$ , 287.1540.

#### 4.12. General Procedure for Conjugation of BODIPY 10.

BODIPY **10** and the biomolecule (peptide, 1-thio- $\beta$ -D-glucose sodium salt or modified biotin-en) were solubilized in anhydrous DMF or in DMSO (0.25–0.5 mL) followed by addition of TEA (0.080 mL). The reaction mixture was covered to prevent penetration of light and allowed to stir at room temperature for 0.5 h. The reaction was subsequently quenched with water and then solubilized in water/MeCN 1:1 and purified using RP-HPLC.

#### 4.13. Synthesis of BODIPY Bioconjugate 11.

BODIPY **10** (0.004 g, 0.0058 mmol), 3PEG-LARLLT (0.016 g, 0.0144 mmol), and TEA (0.080 mL) were used. The conjugate was purified by RP-HPLC (50% A for 5 min, 30% A to 10% A over 13 min, 10% A to 50% A over 2 min at a flow rate of 4 mL/min) with  $t_R$  = 12.405 min. The desired fractions were pooled and lyophilized to afford conjugate **11** as a light blue solid (0.0082 mg, 90%). mp 151–152 °C;  $^1\text{H}$  NMR (500 MHz,  $\text{DMSO}-d_6$ ):  $\delta$  8.11–7.94 (m, 5H), 7.86 (dd,  $J$  = 11.1, 7.9 Hz, 3H), 7.75 (d,  $J$  = 8.4 Hz, 2H), 7.68 (d,  $J$  = 8.4 Hz, 2H), 7.49–7.38 (m, 3H), 7.25 (q,  $J$  = 6.7 Hz, 3H), 7.05 (d,  $J$  = 16.9 Hz, 3H), 6.90 (s, 2H), 4.27 (dp,  $J$  = 28.7, 7.3 Hz, 6H), 4.09–3.97 (m, 3H), 3.82 (s, 3H), 3.68 (t,  $J$  = 5.7 Hz, 6H), 3.61 (q,  $J$  = 6.6, 5.7 Hz, 14H), 3.08 (q,  $J$  = 6.6 Hz, 2H), 2.46–2.29 (m, 4H), 1.63 (dtq,  $J$  = 26.2, 13.5, 7.1 Hz, 5H), 1.54–1.47 (m, 4H), 1.47 (s, 1H), 1.43 (t,  $J$  = 7.9 Hz, 4H), 1.20 (d,  $J$  = 7.1 Hz, 4H), 1.00 (d,  $J$  = 6.3 Hz, 3H), 0.85 (ddd,  $J$  = 23.3, 6.4, 3.8 Hz, 18H), 0.77 (s, 1H). HRMS (MALDI-TOF)  $m/z$ : calcd for  $\text{C}_{79}\text{H}_{103}\text{BF}_2\text{N}_{15}\text{O}_{13}\text{S}_2^+$ , 1581.739; found  $[\text{M}]^+$ , 1581.681.

#### 4.14. Synthesis of BODIPY Bioconjugate 12.

Conjugate **11** (0.003 g, 0.0019 mmol) and 1-thio- $\beta$ -D-glucose sodium salt (0.0021 g, 0.0095 mmol) and TEA (0.006 mL) were used. The resulting conjugate was purified by RP-HPLC (50% A for 5 min, 30% A to 10% A over 13 min, 10% A to 50% A over 2 min at a flow rate of 4 mL/min) with  $t_R$  = 12.296 min. The desired fractions were pooled and lyophilized to afford conjugate **12** as a light blue solid (2.80 mg, 83%). mp °C;  $^1\text{H}$  NMR (500 MHz,  $\text{DMSO}-d_6$ ):  $\delta$  8.03 (dd,  $J$  = 32.4, 15.2 Hz, 5H), 7.88 (d,  $J$  = 8.8 Hz, 2H), 7.80–7.72 (m, 3H),

7.70 (s, 2H), 7.56 (s, 1H), 7.45–7.34 (m, 4H), 7.26 (s, 2H), 7.06 (d,  $J = 14.9$  Hz, 3H), 6.90 (dd,  $J = 15.8, 7.9$  Hz, 3H), 6.43 (d,  $J = 6.8$  Hz, 2H), 4.83 (s, 1H), 4.31 (dd,  $J = 15.5, 8.0$  Hz, 3H), 4.27–4.20 (m, 3H), 4.10–4.00 (m, 4H), 3.83 (s, 3H), 3.57 (s, 6H), 3.52 (s, 8H), 3.09 (d,  $J = 7.0$  Hz, 2H), 2.27 (s, 1H), 1.61 (dt,  $J = 15.5, 8.1$  Hz, 4H), 1.49 (dt,  $J = 28.5, 13.1$  Hz, 9H), 1.27–1.18 (m, 6H), 1.00 (d,  $J = 6.2$  Hz, 3H), 0.85 (ddt,  $J = 21.6, 10.3, 5.7$  Hz, 19H). HRMS (MALDI-TOF)  $m/z$ : calcd for  $C_{85}H_{115}BF_2N_{15}O_{18}S_3^+$ , 1777.780; found  $[M]^+$ , 1777.834.

#### 4.15. Synthesis of BODIPY Bioconjugate 13.

Conjugate **11** (0.003 g, 0.0019 mmol), modified biotin-en (0.0027 g, 0.0095 mmol), and TEA (0.006 mL) were used. The resulting conjugate was purified by RP-HPLC (50% A for 5 min, 30% A to 10% A over 13 min, 10% A to 50% A over 2 min at a flow rate of 4 mL/min) with  $t_R = 12.217$  min. The desired fractions were pooled and lyophilized to afford conjugated **13** as a light blue solid (1.59 mg, 45%). mp 195–196 °C;  $^1H$  NMR (500 MHz, DMSO- $d_6$ ):  $\delta$  8.08–7.92 (m, 3H), 7.87 (t,  $J = 9.4$  Hz, 2H), 7.75 (d,  $J = 8.4$  Hz, 1H), 7.69 (d,  $J = 8.1$  Hz, 1H), 7.46 (t,  $J = 5.9$  Hz, 1H), 7.41 (d,  $J = 8.3$  Hz, 1H), 7.20 (s, 1H), 7.06 (d,  $J = 17.2$  Hz, 2H), 6.89 (d,  $J = 17.9$  Hz, 1H), 6.49 (s, 3H), 6.43 (d,  $J = 7.7$  Hz, 1H), 4.86 (d,  $J = 4.9$  Hz, 1H), 4.28 (dp,  $J = 28.4, 7.4$  Hz, 4H), 4.05 (ddd,  $J = 26.2, 9.5, 4.0$  Hz, 2H), 3.83 (s, 2H), 3.69 (s, 1H), 3.64–3.56 (m, 4H), 3.54–3.46 (m, 4H), 3.08 (t,  $J = 6.7$  Hz, 2H), 2.37–2.32 (m, 1H), 1.61 (dq,  $J = 12.5, 6.4$  Hz, 3H), 1.48 (ddq,  $J = 19.7, 13.2, 8.0, 6.4$  Hz, 7 h), 1.27–1.15 (m, 4 h), 1.00 (d,  $J = 6.2$  Hz, 2H), 0.86 (dt,  $J = 24.0, 5.5$  Hz, 13H). HRMS (MALDI-TOF)  $m/z$ : calcd for  $C_{91}H_{125}BF_2N_{19}O_{15}S_3^+$ , 1867.886; found  $[M]^+$ , 1867.919.

#### 4.16. Synthesis of BODIPY Bioconjugate 14.

BODIPY **10** (0.003 g, 0.0043 mmol), 1-thio- $\beta$ -D-glucose sodium salt (0.0024 g, 0.011 mmol), and TEA (0.006 mL) were used. The resulting conjugate was purified by RP-HPLC (50% A for 5 min, 30% A to 10% A over 13 min, 10% A to 50% A over 2 min at a flow rate of 4 mL/min) with  $t_R = 22.505$  min. The desired fractions were pooled and lyophilized to afford conjugate **14** as a light blue solid (2.02 mg, 43%). mp 262–263 °C;  $^1H$  NMR (500 MHz, DMSO- $d_6$ ):  $\delta$  7.79 (d,  $J = 8.0$  Hz, 4H), 7.62 (d,  $J = 8.0$  Hz, 4H), 7.53 (d,  $J = 7.8$  Hz, 2H), 7.28 (p,  $J = 7.0$  Hz, 4H), 6.92 (s, 3H), 6.49 (s, 5H), 6.45 (d,  $J = 8.1$  Hz, 2H), 3.83 (s, 7H), 3.29 (s, 8H), 2.09 (s, 10H). HRMS (MALDI-TOF)  $m/z$ : calcd for  $C_{51}H_{49}BF_2N_4O_{12}S_4^+$ , 1085.232; found  $[M]^+$ , 1085.410.

#### 4.17. Synthesis of BODIPY Bioconjugate 15.

BODIPY **10** (0.003 g, 0.0019 mmol), modified biotin-en, and TEA (0.006 mL) were used. The resulting conjugate was purified by RP-HPLC (50% A for 5 min, 30% A to 10% A over 13 min, 10% A to 50% A over 2 min at a flow rate of 4 mL/min) with  $t_R = 11.980$  min. The desired fractions were pooled and lyophilized to afford compound **15** as a light blue solid (0.602 mg, 11%). mp 210–211 °C;  $^1H$  NMR (500 MHz, DMSO- $d_6$ ):  $\delta$  9.92 (s, 1H), 8.08 (s, 1H), 7.94 (s, 1H), 7.70 (t, 8.7 Hz, 4H), 7.57 (s, 2H), 7.25 (s, 4H), 6.91 (s, 2H), 6.62–6.17 (m, 6H), 4.28 (s, 1H), 4.11 (s, 1H), 3.83 (s, 4H), 3.29 (s, 24H), 2.09 (s, 18H). HRMS (MALDI-TOF)  $m/z$ : calcd for  $C_{63}H_{69}BF_2N_{12}O_6S_4^+$ , 1265.444; found  $[M]^+$ , 1265.293.

#### 4.18. X-Ray Crystallography.

X-ray data were collected at low temperature with Mo  $K\alpha$  radiation on Bruker Kappa Apex-II DUO diffractometer. Crystal data: **10** C<sub>39</sub>H<sub>25</sub>BF<sub>2</sub>N<sub>4</sub>O<sub>2</sub>S<sub>2</sub>  $M_r = 694.56$ , triclinic,  $a = 8.9803(4)$  Å,  $b = 12.7742(6)$  Å,  $c = 14.8284(8)$  Å,  $\alpha = 100.414(2)^\circ$ ,  $\beta = 98.207(2)^\circ$ ,  $\gamma = 93.875(2)^\circ$ ,  $T = 180$  K, space group  $P\bar{1}$ ,  $Z = 2$ , 20 404 reflections measured, 5945 independent ( $R_{\text{int}} = 0.029$ ),  $\theta_{\text{max}} = 69.3^\circ$ ,  $R = 0.036$ .

#### 4.19. Steady-State Absorption and Fluorescence Spectroscopy.

Spectroscopic properties of BODIPY conjugates were determined in DMSO. All experiments were carried out within 3 h of solution preparation at room temperature (23–25 °C) using a 10 mm path length spectrophotometric cell. All absorption spectra were measured using a Varian Cary 50 Bio UV/vis spectrophotometer (Agilent Technologies, Santa Clara CA). Emission spectra were recorded on a PerkinElmer LS 55 fluorescence spectrometer (PerkinElmer, Waltham MA). The fluorescence quantum yields ( $\Phi_F$ ) were determined using a secondary standard method using methylene blue ( $\Phi_F = 0.035$ ) as the reference.<sup>41</sup>

#### 4.20. Surface Plasmon Resonance.

Surface plasmon resonance studies were conducted using immobilized EGFR on a CM5 sensor chip via standard amine coupling with a Biacore X100 (GE Healthcare Life Sciences, Marlborough MA). Running buffer used was 4% DMSO in 1× HBS-EP + [0.01 M N-(2-hydroxyethyl)-piperazine- $N'$ -ethanesulfonic acid, 0.15 M NaCl, 3 mM ethylenediaminetetraacetic acid (EDTA), 0.005% Tween, pH 7.5] (GE Healthcare Biosciences), at a flow rate of 5  $\mu\text{L}/\text{min}$ . All solutions were prepared in running buffer and filtered using a 0.45  $\mu\text{m}$  filter. All SPR sensorgrams measure association and dissociation rates of analytes at concentrations of 0–300  $\mu\text{M}$  performed at 25 °C.

#### 4.21. Competitive Binding Studies.

Cells SW-480, HT-29, DLD-1, and LoVo were grown to confluency. About 10 000 cells of each cell line were coated in a 96 well tissue culture black plate and incubated overnight at 37 °C with 5% CO<sub>2</sub>. After 24 h, the medium was removed, and different concentrations (0.25–100  $\mu\text{M}$ ) of cyclo(K(N<sub>3</sub>)larIt)<sup>32</sup> with a constant concentration (50  $\mu\text{M}$ ) of conjugate **12** or **14** was added to the wells in triplicate. Phosphate-buffered saline (PBS) was used for dilution of compounds. The plate was then covered in aluminum foil and incubated at 37 °C with 5% CO<sub>2</sub>. After 45 min, each well was washed twice with 100  $\mu\text{L}$  of PBS, and fluorescence was determined with a microplate reader using an excitation wavelength of 647 nm and an emission wavelength of 683 nm. Autofluorescence values were subtracted from each well. A plot of concentrations versus relative fluorescence was plotted. Results are expressed as  $\pm$ S.D.

#### 4.22. Molecular Modeling and Docking.

The structure of compounds and conjugates were generated using Insight II (BIOVIA, San Diego CA) molecular modeling software on a Linux workstation. Generated 3D structures were subjected to molecular dynamics (MD) at 900 K and each structure was subjected to

simulated annealing procedure by decreasing the temperature from 900 to 300 K in steps of 100 K. At each step, 10 ps MD simulations were carried out. Structures obtained after 300 K dynamics were energy minimized. The resulting structure was used for docking studies. Docking studies were conducted using AutoDock<sup>39</sup> with AutoDock tools. Before docking calculations were performed, the boron atom was replaced with a carbon atom in the conjugate, as boron parameters are not validated in the AutoDock 4. The EGFR protein structure was downloaded from protein data bank (PDB ID 1nql).<sup>40</sup> Docking calculations were performed as described before in our earlier reports.<sup>21</sup> Briefly, a grid box (AutoDock tools 4) was created around domain I of ECD of EGFR and compounds **10**, **11**–**15** were docked to EGFR using Lamarckian genetic algorithm, and 10 million energy evaluations were performed. For conjugate **11** docking, a grid box was created between the domain I and II of EGFR and docking calculations were performed using 10 million energy evaluations. Final docked structures were represented using PyMol software (Schrödinger LLC, Portland OR).

#### 4.23. Cell Studies.

All cell culture media and reagents were purchased from Invitrogen unless otherwise stated. Human colorectal adenocarcinoma cell lines HT-29 (ATCC HTB-38), SW480 (ATCC CCL-227) and LoVo (ATCC CCL-229) were purchased from ATCC and maintained at 37 °C under 5% CO<sub>2</sub> in McCoy's 5A medium, Leibovitz's L-15 medium and Ham's F-12K (Kaighn's) medium/Dulbecco's modified Eagle medium, respectively, all augmented with 10% fetal bovine serum (FBS) and 1% penicillin–streptomycin (P/S). Working stock solutions of BODIPY conjugates were prepared at 32 mM in 4% DMSO and 1% Cremophor-EL in Dulbecco's phosphate-buffered saline (1× PBS).

#### 4.24. Time-Dependent Cellular Uptake.

HT-29 cells were plated in a Corning Costar 96-well plate and were allowed to grow 48 h to reach approximately 7500 cells per well. Working stock solutions of BODIPY conjugates were diluted with McCoy's 5A medium augmented with 10% FBS and 1% P/S to 20  $\mu$ M. Cells were exposed to BODIPY conjugates at a final concentration of 10  $\mu$ M at 0, 1, 2, 4, 8, and 24 h time intervals. At the end of the incubation period, the loading medium was removed, and cells were washed with 200  $\mu$ L of 1× PBS and then solubilized with 100  $\mu$ L of 0.25% Triton X-100 (Calbiochem, San Diego CA) in 1× PBS. The CyQUANT Cell Proliferation Assay Kit (Invitrogen, Carlsbad CA) was utilized for cell quantification. BODIPY concentrations were determined by fluorescence intensity at 640/680 nm (excitation/emission) using a FLUOstar OPTIMA microplate reader (BMG Labtech, Cary NC). The cellular uptake is expressed in nM of compound per cell.

#### 4.25. Dark Cytotoxicity.

HT-29 cells were plated as previously described above and allowed to incubate for 48 h. Subsequently, cells were exposed to BODIPY conjugate at increasing concentrations (6.25, 12.5, 25, 50, 100, and 200  $\mu$ M) and then incubated overnight (20–24 h) at 37 °C under 5% CO<sub>2</sub>. Immediately following incubation, the loading medium was removed and cells were washed in triplicate with media to remove any residual BODIPY compound. Cells were then

fed McCoy's 5A medium containing 20% CTB (Promega, Madison WI) and incubated for 4 h at 37 °C under 5% CO<sub>2</sub>. Cell viability was determined by fluorescence intensity at 570/615 nm using a FLUOstar OPTIMA microplate reader. Cell dark toxicity is expressed as a percentage of viable cells.

#### 4.26. Phototoxicity.

HT-29 cells were plated as previously described above and allowed to incubate for 48 h. Subsequently, cells were exposed to BODIPY conjugate at increasing concentrations (3.125, 6.25, 12.5, 25, 50, and 100  $\mu$ M) and then incubated overnight (20–24 h) at 37 °C under 5% CO<sub>2</sub>. Immediately after incubation, the loading medium was removed and cells were washed in triplicate with media to remove any residual BODIPY compound. Cells were then fed McCoy's 5A medium and exposed to light using a 600W Quartz Tungsten Halogen lamp (Newport Corporation, Irvine CA) to generate a light dose of 1.5 J/cm<sup>2</sup>. Cells were exposed for 20 min while the plate rested on an EchoTherm IC50 chilling/heating plate (Torrey Pines Scientific, Carlsbad CA) set to 5 °C to maintain ambient temperature. Following light exposure, cells were incubated for 24 h, after which the media were removed and replaced with 20% CTB in McCoy's 5A medium and subsequently incubated for 4 h. Cell viability was determined by fluorescence intensity at 570/615 nm using a FLUOstar OPTIMA microplate reader. Cell phototoxicity is expressed as a percentage of viable cells.

#### 4.27. Microscopy.

HT-29 cells were plated in a 35 mm tissue culture dish (CELLTREAT, Pepperell MA) and were allowed to grow overnight. Cells were exposed to BODIPY conjugates at a final concentration of 10  $\mu$ M then immediately incubated at 37 °C for 15 min. Following the incubation period, the loading media were removed and the cells were washed with 1  $\times$  PBS in triplicate. Cells were imaged submerged/immersed in 1 $\times$  PBS, 0.25% Triton X-100. Images were captured/acquired using a Leica DM RXA2 (DM6Bs) motorized upright confocal laser scanning microscope (Leica; Wetzlar, Germany) equipped with a water immersion objective and fitted with standard Texas Red, FITC, DAPI, GFP, YFP, TRITC, and Cy5LP filter cubes (Chroma Technology Corporation, Bellows Falls VA).

#### 4.28. Animal Studies.

For animal studies, athymic nu/nu mice (Charles River Laboratories, Wilmington MA) were purchased at 6 weeks of age and quarantined for 1 week. Subsequently, the human colorectal adenocarcinoma HT-29 cell line (ATCC; Manassas, VA) was implanted subcutaneously in the lower right flank. Initially, HT-29 cells were cultured in a McCoy's 5A medium containing 10% FBS (Atlanta Biologicals; Flowery Branch, GA) to approximately 75% confluence, treated with 0.25% (w/v) trypsin—0.53 mM EDTA solution, concentrated via centrifugation, and resuspended in Dulbecco's PBS before injection. The cells were incubated at 37 °C and 5% CO<sub>2</sub> under humidified conditions. Each of the mice was injected with 5  $\times$  10<sup>6</sup> cells in 0.1 mL PBS. Tumors were allowed to develop until palpable (approximately 2 weeks), after which mice were subjected to lateral tail vein injection of BODIPY conjugates at 2 mM in 10% DMSO and 5% Cremophor EL in Dulbecco's PBS. After injection, the mice were observed for acute adverse responses and then anesthetized using 3% isoflurane for imaging. Fluorescence imaging was performed at 10 min after

injection and at 1, 2, 3, 4, and 5 days using a Spectral AMI optical imaging system (Spectral Instruments Imaging; Tucson, AZ) set at excitation 640 nm and emission 690 nm. All experimental protocols involving live animals were reviewed and approved by the Institutional Animal Care and Use Committee (IACUC) of LSU.

## Supplementary Material

Refer to Web version on PubMed Central for supplementary material.

## ACKNOWLEDGMENTS

Computational studies were performed using HPC resources at Louisiana State University, Baton Rouge via LONI. BBC core of LBRN is acknowledged for the use of the computational facility.

### Funding

This work was supported by the National Institutes of Health, grant number R01 CA179902, and the National Science Foundation, grant number 1800126.

## ABBREVIATIONS

<b>3PEG</b>	tri(ethylene) glycol
<b>Boc</b>	<i>tert</i> -butoxycarbonyl
<b>BODIPY</b>	4,4-difluoro-4-bora-3a,4a-diaza- <i>s</i> -indacene
<b>CrEL</b>	Cremo-phor EL
<b>CTB</b>	CellTiter-Blue
<b>DBU</b>	1,8-diazabicyclo[5.4.0]-undec-7-ene
<b>DCM</b>	dichloromethane
<b>DDQ</b>	2,3-dichloro-5,6-dicyano-1,4-benzoquinone
<b>DIPEA</b>	diisopropylethylamine
<b>DMF</b>	dimethylformamide
<b>ECD</b>	extracellular domain
<b>EGFR</b>	epidermal growth factor receptor
<b>en</b>	ethylenediamine
<b>ESI-TOF</b>	electrospray ionization-time of flight
<b>EtOAc</b>	ethyl acetate
<b>EtOH</b>	ethanol
<b>Fmoc</b>	fluorenylmethyloxycarbonyl

<b>HBTU</b>	<i>O</i> -benzotriazole- <i>N,N,N',N'</i> -tetramethyl-uronium-hexa-fluorophosphate
<b>HOAt</b>	1-hydroxy-7-azabenzotriazole
<b>HOBt</b>	1-hydroxybenzotriazole
<b>HRMS</b>	high resolution mass spectrometry
<b>HSQC</b>	heteronuclear single quantum correlation
<b>IR</b>	infrared
<b>iv</b>	intravenous
<b>MALDI-TOF MS</b>	matrix assisted laser desorption ionization-time of flight mass spectrometry
<b>MeOH</b>	methanol
<b>MQ</b>	Milli-Q
<b>NIR</b>	near infrared
<b>NMR</b>	nuclear magnetic resonance
<b>P (dppf)Cl<sub>2</sub></b>	[1,1'-bis-(diphenylphosphino)ferrocene]dichloropalladium (II)
<b>rt</b>	room temperature
<b>RTK</b>	receptor tyrosine kinase
<b>RP-HPLC</b>	reversed phase-high performance liquid chromatography
<b>SPPS</b>	solid-phase peptide synthesis
<b>TEA</b>	triethyl-amine
<b>TDP</b>	1,1'-thiocarbonyldi-2(1 <i>H</i> )-pyridone
<b>TFA</b>	tri-fluoroacetic acid
<b>TGF-<math>\alpha</math></b>	transforming growth factor- $\alpha$
<b>THF</b>	tetrahydrofuran
<b>TIPS</b>	triisopropylsilane
<b>TKI</b>	tyrosine kinase inhibitor
<b>TLC</b>	thin layer chromatography
<b>TsOH</b>	<i>p</i> -toluenesulfonic acid
<b>UV-vis</b>	ultraviolet-visible



## ■ REFERENCES

- (1). James ML; Gambhir SS A Molecular Imaging Primer: Modalities, Imaging Agents, and Applications. *Physiol. Rev* 2012, 92, 897–965. [PubMed: 22535898]
- (2). Willmann JK; van Bruggen N; Dinkelborg LM; Gambhir SS Molecular Imaging in Drug Development. *Nat. Rev. Drug Discovery* 2008, 7, 591. [PubMed: 18591980]
- (3). Park SH; Lee SS; Choi EK; Kim SY; Yang S-K; Kim JH; Ha HK Flat Colorectal Neoplasms: Definition, Importance, and Visualization on CT Colonography. *Am. J. Roentgenol* 2007, 188, 953–959. [PubMed: 17377029]
- (4). NIH National Cancer Institute. <https://www.cancer.gov/types/colorectal> (accessed Jul 18, 2018).
- (5). Li S; Buchbinder E; Wu L; Bjorge JD; Fujuta DJ; Zhu S EGFR and HER2 Levels are Frequently Elevated in Colon Cancer Cells. *Discover. Rep* 2014, 1, No. e1.
- (6). Paganin-Gioanni A; Bellard E; Paquereau L; Ecochard V; Golzio M; Teissie J Fluorescence Imaging Agents in Cancerology. *Radiol. Oncol* 2010, 44, 142–148. [PubMed: 22933906]
- (7). Radinsky R; Risin S; Fan D; Dong Z; Bielenberg D; Bucana CD; Fidler IJ Level and Function of Epidermal Growth Factor Receptor Predict the Metastatic Potential of Human Colon Carcinoma Cells. *Clin. Cancer Res* 1995, 1, 19–31. [PubMed: 9815883]
- (8). Yang J-L; Qu XJ; Russell PJ; Goldstein D Regulation of Epidermal Growth Factor Receptor in Human Colon Cancer Cell Lines by Interferon  $\alpha$ . *Gut* 2004, 53, 123–129. [PubMed: 14684586]
- (9). Zhao N; Williams TM; Zhou Z; Fronczek FR; Sibrian-Vazquez M; Jois SD; Vicente MGH Synthesis of BODIPY-Peptide Conjugates for Fluorescence Labeling of EGFR Over-expressing Cells. *Bioconjugate Chem.* 2017, 28, 1566–1579.
- (10). Barton DHR; Zard SZ A New Synthesis of Pyrroles from Nitroalkenes. *J. Chem. Soc. Chem. Commun* 1985, 16, 1098–1100.
- (11). Ka J-W; Lee C-H Optimizing the Synthesis of 5,10-disubstituted Tripyrromethanes. *Tetrahedron Lett.* 2000, 41, 4609–4613.
- (12). Rohand T; Qin W; Boens N; Dehaen W Palladium-Catalyzed Coupling Reactions for the Functionalization of BODIPY Dyes with Fluorescence Spanning the Visible Spectrum. *Eur. J. Org. Chem* 2006, 2006, 4658–4663.
- (13). Loudet A; Burgess K BODIPY Dyes and Their Derivatives: Syntheses and Spectroscopic Properties. *Chem. Rev* 2007, 107, 4891. [PubMed: 17924696]
- (14). Tang Y; Zeng X; Liang J Surface Plasmon Resonance: An Introduction to a Surface Spectroscopy Technique. *J. Chem. Educ* 2010, 87, 742–746. [PubMed: 21359107]
- (15). Patching SG Surface plasmon resonance spectroscopy for characterisation of membrane protein-ligand interactions and its potential for drug discovery. *Biochim. Biophys. Acta, Biomembr* 2014, 1838, 43–55.
- (16). Hao E; Jensen TJ; Vicente MGH Synthesis of porphyrin-carbohydrate conjugates using “click” chemistry and their preliminary evaluation in human HEP2 cells. *J. Porphyrins Phthalocyanines* 2009, 13, 51–59.
- (17). Nguyen AL; Griffin KE; Zhou Z; Fronczek FR; Smith KM; Vicente MGH Syntheses of 1,2,3-Triazole-BODIPYs Bearing up to Three Carbohydrate Units. *New J. Chem* 2018, 42, 8241–8246.
- (18). Fuhrhop JH; Demoulin C; Boettcher C; Koenig J; Siggel U Chiral Micellar Porphyrin Fibers with 2-Aminoglycosamide Head Groups. *J. Am. Chem. Soc* 1992, 114, 4159–4165.
- (19). Chen X; Hui L; Foster DA; Drain CM Efficient Synthesis and Photodynamic Activity of Porphyrin-Saccharide Conjugates: Targeting and Incapacitating Cancer Cells. *Biochemistry* 2004, 43, 10918–10929. [PubMed: 15323552]
- (20). Laville I; Pigaglio S; Blais J-C; Doz F; Loock B; Maillard P; Grierson DS; Blais J Photodynamic Efficiency of Diethylene Glycol-Linked Glycoconjugated Porphyrins in Human Retinoblastoma Cells. *J. Med. Chem* 2006, 49, 2558–2567. [PubMed: 16610799]
- (21). Williams TM; Sable R; Singh S; Vicente MGH; Jois SD Peptide Ligands for Targeting the Extracellular Domain of EGFR: Comparison Between Linear and Cyclic Peptides. *Chem. Biol. Drug Des* 2018, 91, 605–619. [PubMed: 29052959]

- (22). Tebbutt N; Pedersen MW; Johns TG Targeting the ERBB Family in Cancer: Couples Therapy. *Nat. Rev. Cancer* 2013, 13, 663. [PubMed: 23949426]
- (23). Burgess AW; Cho H-S; Eigenbrot C; Ferguson KM; Garrett TPJ; Leahy DJ; Lemmon MA; Sliwkowski MX; Ward CW; Yokoyama S An Open-and-Shut Case? Recent Insights into the Activation of EGF/ErbB Receptors. *Mol. Cell* 2003, 12, 541 – 552. [PubMed: 14527402]
- (24). Schlessinger J Ligand-Induced, Receptor-Mediated Dimerization and Activation of EGF Receptor. *Cell* 2002, 110, 669–672. [PubMed: 12297041]
- (25). Zhang X; Gureasko J; Shen K; Cole PA; Kuriyan J An Allosteric Mechanism for Activation of the Kinase Domain of Epidermal Growth Factor Receptor. *Cell* 2006, 125, 1137–1149. [PubMed: 16777603]
- (26). Ulrich G; Zissel R; Harriman A The Chemistry of Fluorescent Bodipy Dyes: Versatility Unsurpassed. *Angew. Chem., Int. Ed* 2008, 47, 1184.
- (27). Pansare VJ; Hejazi S; Faenza WJ; Prud'homme RK Review of Long-Wavelength Optical and NIR Imaging Materials: Contrast Agents, Fluorophores, and Multifunctional Nano Carriers. *Chem. Mater* 2012, 24, 812–827. [PubMed: 22919122]
- (28). Li Z; Zhao R; Wu X; Sun Y; Yao M; Li J; Xu Y; Gu J Identification and Characterization of a Novel Peptide Ligand of Epidermal Growth Factor Receptor for Targeted Delivery of Therapeutics. *FASEB J.* 2005, 19, 1978–1985. [PubMed: 16319141]
- (29). Fontenot KR; Ongarora BG; LeBlanc LE; Zhou Z; Jois SD; Vicente MGH Targeting of the Epidermal Growth Factor Receptor with Mesoporphyrin IX-Peptide Conjugates. *J. Porphyrins Phthalocyanines* 2016, 20, 352.
- (30). Ongarora BG; Fontenot KR; Hu X; Sehgal I; Satyanarayana-Jois SD; Vicente MGH Phthalocyanine-Peptide Conjugates for Epidermal Growth Factor Receptor Targeting. *J. Med. Chem* 2012, 55, 3725. [PubMed: 22468711]
- (31). Song S; Liu D; Peng J; Deng H; Guo Y; Xu LX; Miller AD; Xu Y Novel Peptide Ligand Directs Liposomes Toward EGF-R High-Expressing Cancer Cells in vitro and in vivo. *FASEB J.* 2009, 23, 1396–1404. [PubMed: 19124558]
- (32). Yu C; Xu Y; Jiao L; Zhou J; Wang Z; Hao E Isoindole-BODIPY Dyes as Red to Near-Infrared Fluorophores. *Chem.—Eur. J* 2012, 18, 6437–6442. [PubMed: 22517763]
- (33). Kiesslich R; Goetz M; Vieth M; Galle PR; Neurath MF Technology Insight: Confocal Laser Endoscopy for in vivo Diagnosis of Colorectal Cancer. *Nat. Clin. Pract. Oncol* 2007, 4, 480. [PubMed: 17657253]
- (34). Liu R; Li H; Gao X; Mi Q; Zhao H; Gao Q Mannose-Conjugated Platinum Complexes Reveals Effective Tumor Targeting Mediated by Glucose Transporter 1. *Biochem. Biophys. Res. Commun* 2017, 487, 34–40. [PubMed: 28385528]
- (35). Bodnar B; Mernyák E; Szabó J; Wölfling J; Schneider G; Zupkó I; Kupihar Z; Kovács L Synthesis and in vitro investigation of potential antiproliferative monosaccharide-d-secoestrone bioconjugates. *Bioorg. Med. Chem. Lett* 2017, 27, 1938–1942. [PubMed: 28343874]
- (36). Meng Q; Fronczek FR; Vicente MGH Synthesis and spectroscopic properties of  $\beta,\beta'$ -dibenzo-3,5,8-triaryl-BODIPYs. *New J. Chem* 2016, 40, 5740–5751.
- (37). Uppal T; Hu X; Fronczek FR; Maschek S; Bobadova-Parvanova P; Vicente MGH Synthesis, Computational Modeling, and Properties of Benzo-Appended BODIPYs. *Chem.—Eur. J* 2012, 18, 3893–3905. [PubMed: 22367756]
- (38). Uppal T; Bhupathiraju NVSDK; Vicente MGH Synthesis and cellular properties of Near-IR BODIPY-PEG and carbohydrate conjugates. *Tetrahedron* 2013, 69, 4687.
- (39). Morris GM; Huey R; Lindstrom W; Sanner MF; Belew RK; Goodsell DS; Olson AJ AutoDock4 and AutoDockTools4: Automated Docking with Selective Receptor Flexibility. *J. Comput. Chem* 2009, 30, 2785. [PubMed: 19399780]
- (40). Ferguson KM; Berger MB; Mendrola JM; Cho H-S; Leahy DJ; Lemmon MA EGF Activates its Receptor by Removing Interactions that Autoinhibit Ectodomain Dimerization. *Mol. Cell* 2003, 11, 507–517. [PubMed: 12620237]
- (41). Olmstead J Calorimetric Determinations of Absolute Fluorescence Quantum Yields. *J. Phys. Chem* 1979, 83, 2581–2584.

*J Med Chem.* Author manuscript; available in PMC 2019 August 14.

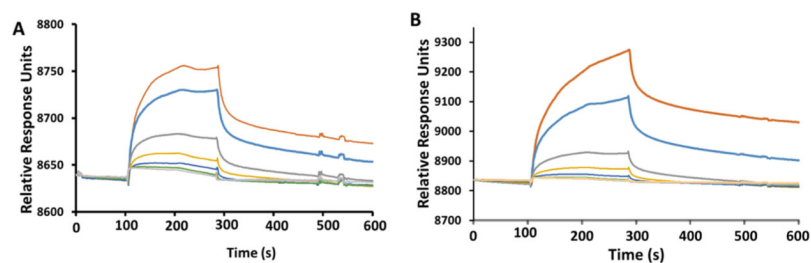


**Figure 2.**

Binding of BODIPYs to EGFR by SPR analysis. BODIPYs (A) 12 and (B) 13 at 250 (orange), 200 (blue), 100 (dark gray), 50  $\mu\text{M}$  (yellow), 25  $\mu\text{M}$  (dark blue), 10  $\mu\text{M}$  (green), 1  $\mu\text{M}$  (light blue), 0.5  $\mu\text{M}$  (pink), 0.25  $\mu\text{M}$  (light gray), and 0  $\mu\text{M}$  (peach) concentrations. EGFR was immobilized and the BODIPYs were used as the analyte to study kinetics of association and dissociation.

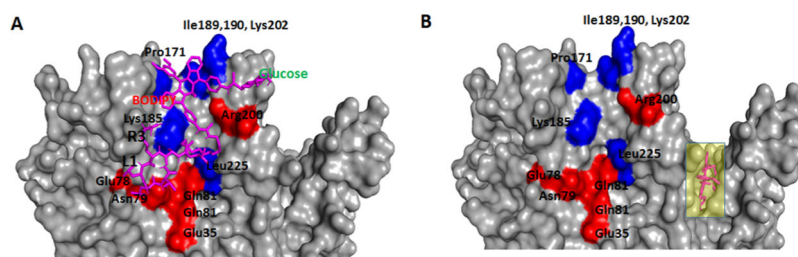


**Figure 3.**

Model of interaction of BODIPYs with EGFR protein using AutoDock. Docking of BODIPYs **12** (A) and **14** (B) were performed with similar parameters and the lowest energy docked structures are represented. The ECD I of EGFR (PDB ID 1NQL)<sup>40</sup> is shown as surface representation and compounds are shown as sticks (magenta). Possible hydrophobic interactions are shown in blue and polar interactions are shown in red. Amino acids of EGFR are represented by a three letter code, and those on peptide are indicated by a single letter code. Note the possible binding of **14** at a different site, shown in a rectangle buried deep inside EGFR, compared with that of **12** on the LARLLT peptide binding site.

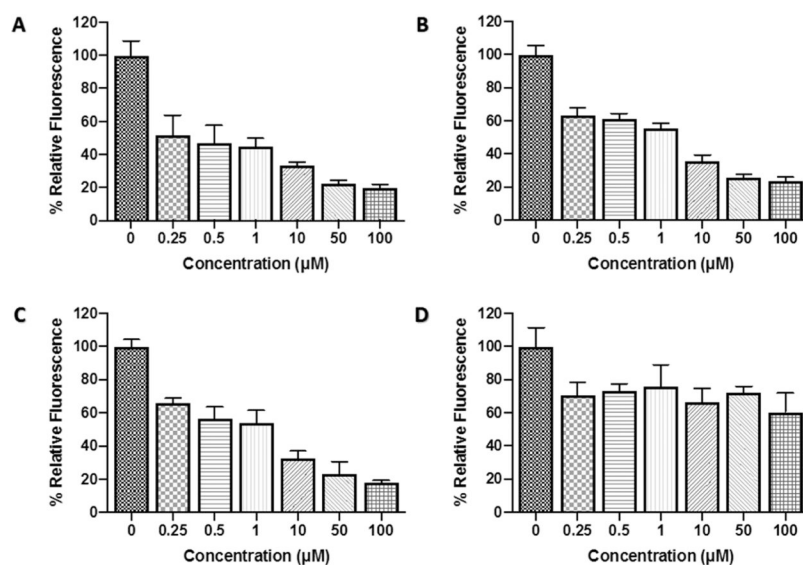


**Figure 4.** Competitive binding of BODIPY 12 (50 μM) with cyclo(K(N<sub>3</sub>)larllt). Binding of **12** to (A) SW480 cells (129% EGFR expression), (B) HT-29 (78% EGFR expression), (C) DLD-1 (37% EGFR expression), (D) LOVO (6% EGFR expression). (Fluorescence without cyclo(K(N<sub>3</sub>)larllt) (0 μM) is considered 100% relative fluorescence where all other fluorescence values reported for increasing concentrations of cyclo(K(N<sub>3</sub>)larllt) are with respect to 100% fluorescence).

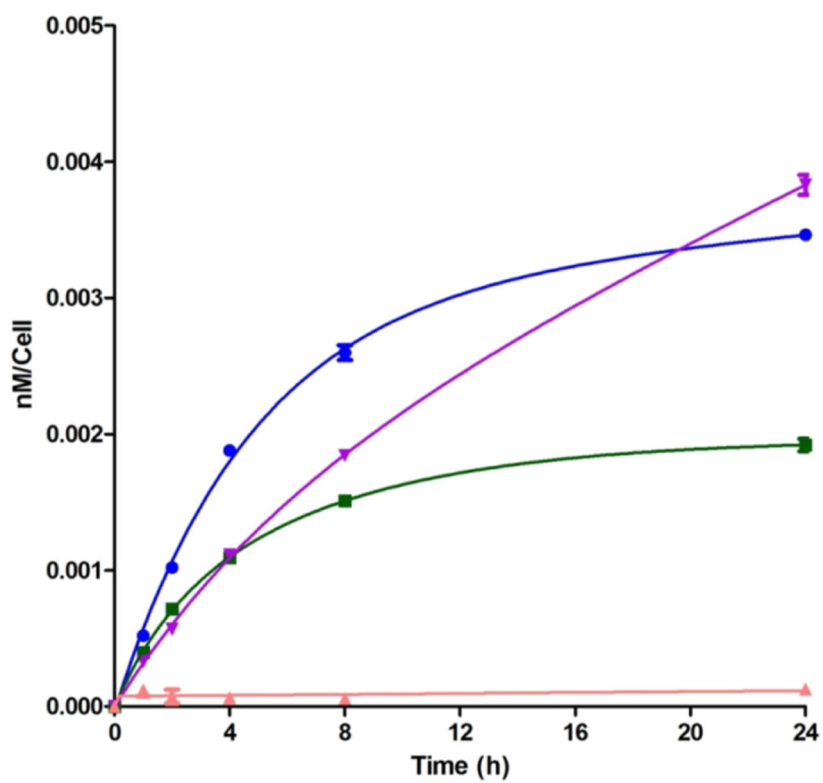


**Figure 5.**  
Time-dependent cellular uptake of compounds **12** (blue), **13** (green), **14** (pink), and **15** (purple) by HT-29 cells over 24 h.



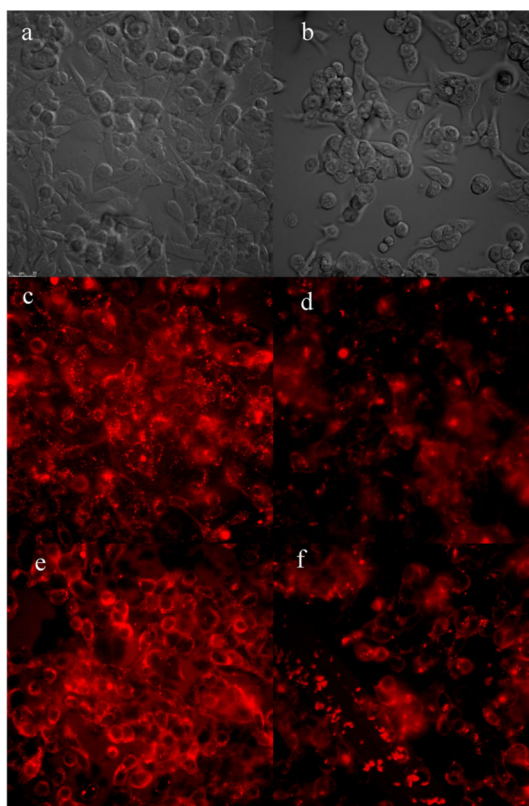


**Figure 6.** Extracellular membrane localization of BODIPYs in SW480 cells (left panels) and LOVO cells (right panels) after 15 min incubation period. (a) Phase contrast for SW480 and (b) LOVO cells, fluorescence of (c,d) **12** and (e,f) **13**. Scale bar: 5  $\mu\text{m}$ .

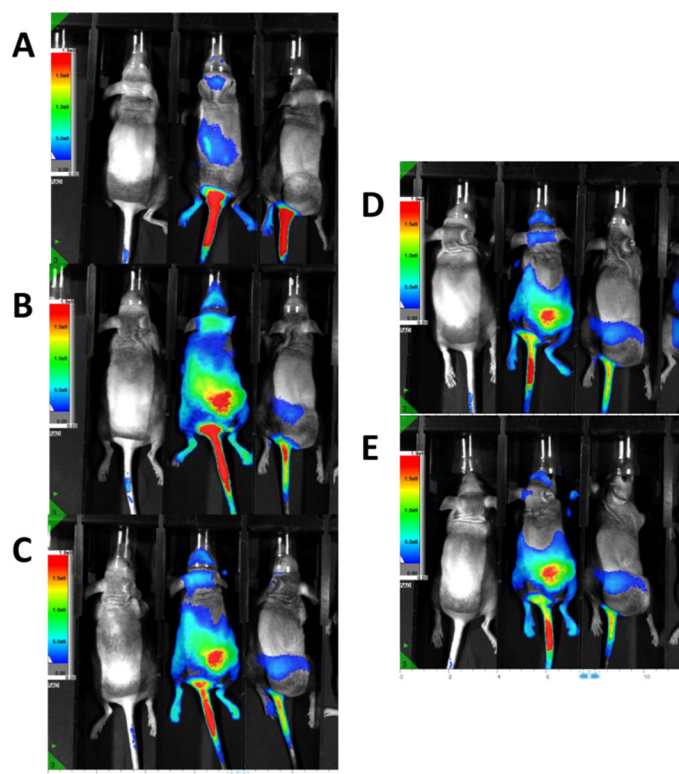
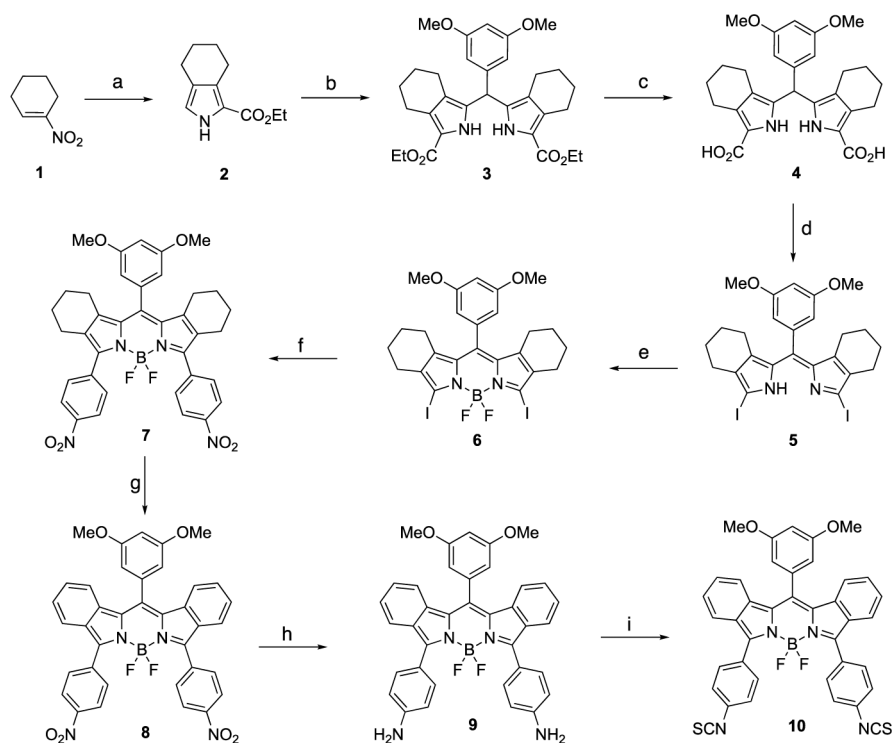
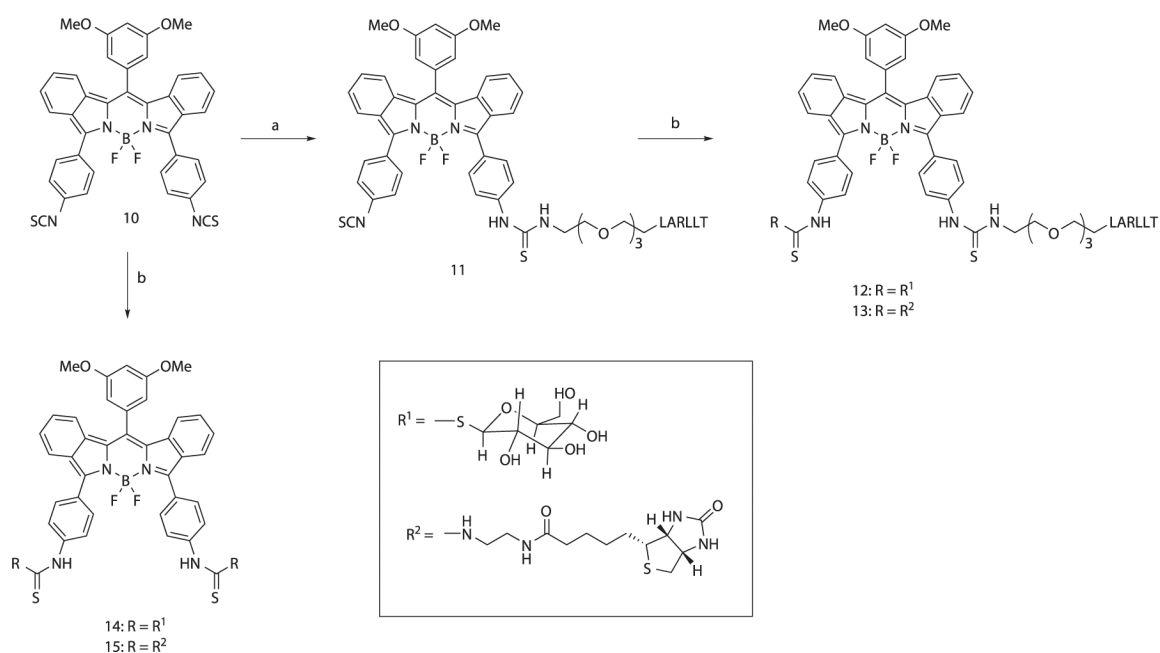


**Figure 7.** Fluorescent images (Ex./Em. 640/690 nm) of nude mice bearing sc tumor implants of HT-29 colorectal adenocarcinoma cells following intravenous (iv) administration of BODIPY conjugates. Negative control (left) and conjugates **12** (center), and **14** (right) at 0 (A), 24 (B), 48 (C), 72 (D), and 96 h (E).



### Scheme 1. Synthesis of Bis(N C S)-BO IPY 10<sup>a</sup>

<sup>a</sup>Reaction conditions: (a) ethyl isocynoacetate, DBU, THF, rt overnight (80%); (b) 3,5-dimethoxybenzaldehyde, *p*-toluenesulfonic acid, *n*-*tert*-butylammonium iodide, dichloromethane (DCM), rt overnight (84%); (c) 1 M KOH, THF, methanol, reflux for 24 h, then 1 M HCl; (d) I<sub>2</sub>, NaHCO<sub>3</sub>, H<sub>2</sub>O/methanol, rt for 72 h; (e) BF<sub>3</sub>·OEt<sub>2</sub>, Et<sub>3</sub>N, DCM, rt for 2 h (68%); (f) 4-nitrophenylboronic acid, Pd(dppf)Cl<sub>2</sub>, K<sub>2</sub>CO<sub>3</sub>, THF/toluene, reflux for 3 h (73–99%); (g) DDQ toluene, reflux for 1.5 h (54–93%); (h) hydrazine, Pd/C, ethanol/THF, reflux for 3 h; (i) TDP, DCM, rt overnight (90%).



**Scheme 2. Synthesis of BODIPY Conjugates 11, 12, 13, 14, and 15<sup>a</sup>**

<sup>a</sup>Reaction conditions: (a) 3PEG-LARLLT, Et<sub>3</sub>N, DMF, rt for 30 min (90%); (b) R<sup>1</sup>-H or R<sup>2</sup>-H, Et<sub>3</sub>N, DMSO, rt for 30 min (11–83%).

**Table 1.**

Spectroscopic Properties of BODIPY Conjugates 11–15 in DMSO and Their Calculated PSA

BODIPY	$\lambda_{\text{max}}$ (nm)		Stokes' shift (nm)	$\epsilon$ (M <sup>-1</sup> cm <sup>-1</sup> )	PSA (Å <sup>2</sup> )	$\Phi_F$
	Abs.	Em.				
11	656	698	39	13 700	393.27	0.37
12	657	696	39	44 200	483.09	0.47
13	650	689	39	72 600	475.20	0.44
14	656	694	38	35 750	231.96	0.47
15	655	695	40	46 700	216.18	0.47

**Table 2.**IC<sub>50</sub> Values for Bioconjugates 12, 13, 14, and 15 Using Cell Titer Blue Assay in Human HT-29 Cells

compound	dark toxicity (IC <sub>50</sub> , $\mu$ M)	phototoxicity (IC <sub>50</sub> , $\mu$ M)
12	>200	94
13	159	>100
14	>200	>100
15	>200	>100